Polarization imaging

MsCV - Module 5 - Sensors & Digitization

Olivier Morel

Laboratory Le2i - UMR CNRS 6306

October 2, 2012

Preamble

Problem statement

As human eye, the conventional cameras are only sensitive to:

- intensity
- hue (wavelength)

Preamble

Problem statement

As human eye, the conventional cameras are only sensitive to:

- intensity
- hue (wavelength)

Solution

Reveal the polarization effects with:

- linear polarizer
- birefringent crystal

Preamble

linear polarizer

- Effect of a polarizer on reflected light:

Preamble

linear polarizer

- Effect of a polarizer on reflected light:

- Effects of a polarizing filter on the sky:

Preamble

Birefringent crystal

Definition

Birefringence, or double refraction, is the decomposition of a ray of light into two rays when it passes through certain anisotropic materials, such as crystals of calcite or boron nitride.

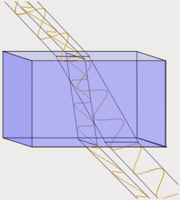

Preamble

Birefringent crystal

Definition

Birefringence, or double refraction, is the decomposition of a ray of light into two rays when it passes through certain anisotropic materials, such as crystals of calcite or boron nitride.

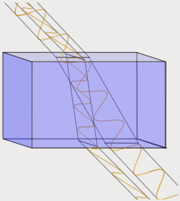

- Birefringent Iceland spar = Viking sun-stone ?
  - Instead of using the polarization skylight, they used the Iceland spar as a depolarizer
  - [Ropars et al., 2011]

Preamble

Human eye can see Polarization !

Haidinger's brush (1844)

- entoptic phenomenon
- macula's dichroism
- birefringence of the cone's outer layer

Preamble

Human eye can see Polarization !

Haidinger's brush (1844)

- entoptic phenomenon
- macula's dichroism
- birefringence of the cone's outer layer

Outline

Polarization contrast measurement

Applications

In many applications of polarization imaging, especially when polarized lighting is used, the polarization contrast measurement is generally sufficient.

Goal

Take 2 different images of an object or a scene with 2 orthogonal views of the polarizer: $I_{||}$ and $I_{\perp}$.

Polarization contrast measurement

Applications

In many applications of polarization imaging, especially when polarized lighting is used, the polarization contrast measurement is generally sufficient.

Goal

Take 2 different images of an object or a scene with 2 orthogonal views of the polarizer: $I_{\parallel}$and $I_{\perp}$.

- The following parameters can be measured:
  - Total light Intensity: $I_{\parallel} + I_{\perp}$
  - Polarization contrast: $I_{\parallel} - I_{\perp}$
  - Polarization contrast ratio: $\frac{I_{\parallel} - I_{\perp}}{I_{\parallel} + I_{\perp}}$
- [Kalayjian et al., 1996, Kalayjian et al., 1997] developed a 1D polarization contrast retina

Outline

Simplified polarization imaging

- In nature, the light is generally not polarized or at least partially linearly polarized:
  - Polarization by reflection
  - Polarization by scattering

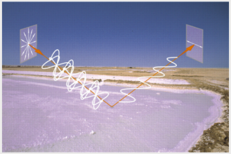

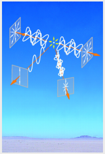

Simplified polarization imaging

- In nature, the light is generally not polarized or at least partially linearly polarized:
  - Polarization by reflection
  - Polarization by scattering

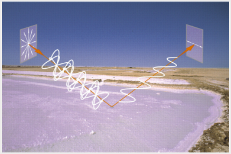

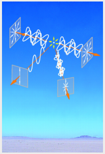

- In this case, three parameters must be estimated:

$$\mathbf{s} = \begin{pmatrix} s_0 \\ s_1 \\ s_2 \\ 0 \end{pmatrix} = \begin{pmatrix} I \\ I\rho\cos 2\varphi \\ I\rho\sin 2\varphi \\ 0 \end{pmatrix}$$

Description of the parameters

(for a partially linearly polarized light)

Total light intensity I

$$I = s_0$$

Degree of polarization ρ

$$\rho = \frac{\sqrt{s_1^2 + s_2^2}}{s_0}$$

Angle of polarization φ

$$\varphi = \frac{1}{2} \arg(s_1 + i s_2),$$

with $i^2 = -1$.

How to measure a part. lin. pol. light ?

Principle

In the case of a part. lin. pol. light a simple rotating polarizer in front of the sensor is sufficient.

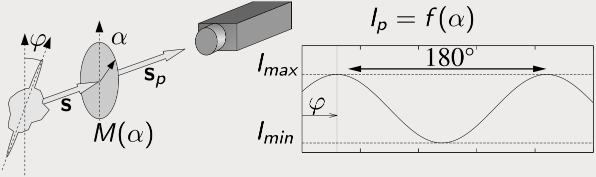

How to measure a part. lin. pol. light ?

Principle

In the case of a part. lin. pol. light a simple rotating polarizer in front of the sensor is sufficient.

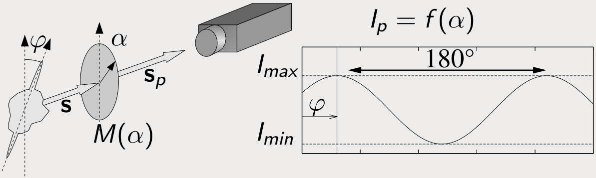

Purpose

For every pixels try to estimate the sinusoid that gives the polarization parameters.

How to measure a part. lin. pol. light ? [Wolff and Andreou, 1995]

Initial idea

A sinusoid is determined by 3 points $\Rightarrow$ 3 images are required to estimate the polarization parameters.

How to measure a part. lin. pol. light ? [Wolff and Andreou, 1995]

Initial idea

A sinusoid is determined by 3 points ⇒ 3 images are required to estimate the polarization parameters.

- [Wolff and Andreou, 1995] suggest taking 3 images corresponding to polarizer orientations of 0°, 45° and 90°:
  - $I = I_0 + I_{90}$
  - $\rho = \frac{I_{90} - I_0}{(I_{90} + I_0)\cos 2\varphi}$
  - $\varphi = \frac{1}{2}\arctan\left(\frac{I_0 + I_{90} - 2I_{45}}{I_{90} - I_0}\right) + 90°$
    if $(I_{90} < I_0)$[if $(I_{45} < I_0)$ $\varphi = \varphi + 90°$ else $\varphi = \varphi - 90°$]

How to measure a part. lin. pol. light ? [Wolff and Andreou, 1995]

Initial idea

A sinusoid is determined by 3 points ⇒ 3 images are required to estimate the polarization parameters.

- [Wolff and Andreou, 1995] suggest taking 3 images corresponding to polarizer orientations of 0°, 45° and 90°:
  - $I = I_0 + I_{90}$
  - $\rho = \frac{I_{90} - I_0}{(I_{90} + I_0)\cos 2\varphi}$
  - $\varphi = \frac{1}{2}\arctan\left(\frac{I_0 + I_{90} - 2I_{45}}{I_{90} - I_0}\right) + 90°$
    if $(I_{90} < I_0)$[if $(I_{45} < I_0)$ $\varphi = \varphi + 90°$ else $\varphi = \varphi - 90°$]
- The proposed configuration leads to a set-up with 2 Twisted Nematic Liquid Crystal [Wolff et al., 1997]

Best configuration

[Tyo, 1998] proved that for a three-channel PVS (Polarization-sensitive Vision/imaging System) the optimum is obtained for a configuration: -60°, 0° and 60°

How to measure a part. lin. pol. light ?

[Wolff and Andreou, 1995]

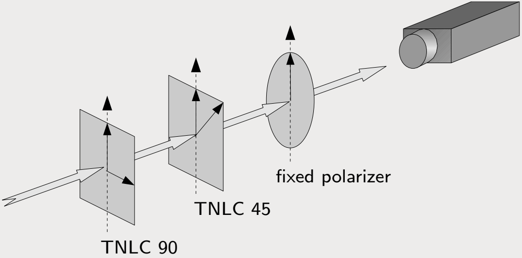

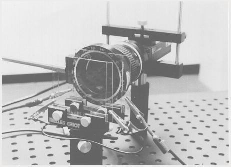

- When an ac voltage is applied across the liquid crystal faces, the helices straighten out so that the plane of linear polarized light is not rotated in this state
- The switching or "relaxation" time of TN liquid crystals is on the order of 1/30 sec.

How to measure a part. lin. pol. light ?

Stereo polarization camera

Main idea

A quite significant speed-up in generating polarization images can be achieved by parallelizing the sensing of polarization components using 2 or more cameras.

- Polarizing beamsplitter:

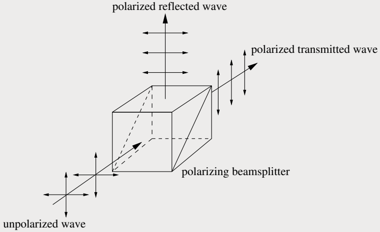

How to measure a part. lin. pol. light ?

Stereo polarization camera

Main idea

A quite significant speed-up in generating polarization images can be achieved by parallelizing the sensing of polarization components using 2 or more cameras.

- Polarizing beamsplitter:

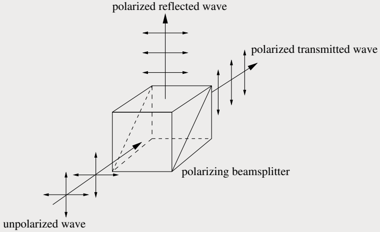

- 7.5 images per second [Wolff and Andreou, 1995]
- automatic calibration process developed by [Terrier and Devlaminck, 2001]

How to measure a part. lin. pol. light ?

[Saito et al., 1999]

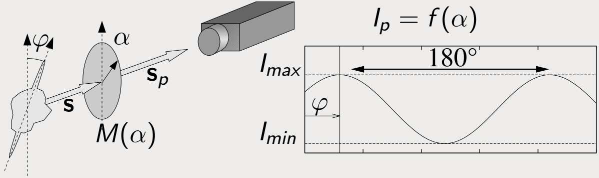

How to measure a part. lin. pol. light ? [Saito et al., 1999]

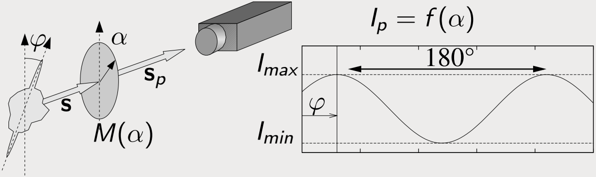

$$\begin{cases} I_p(\alpha) = \frac{I_{max}+I_{min}}{2}\left(1 + \frac{I_{max}-I_{min}}{I_{max}+I_{min}}\cos(2\alpha - 2\varphi)\right) \\ I_p(\alpha) = \frac{I}{2}\left(1 + \rho \cdot \cos(2\alpha - 2\varphi)\right) \end{cases}$$

1. take several images with different orientations of the polarizer
2. for every pixels
   - take the max and the min to compute I and ρ
   - when the minimum occurs, the angle of polarization φ is given by the angle of the linear polarizer α.

Methods for computing the parameters

- Example of a sphere lit with a diffuse dome light:

AOP φ			
DOP ρ			

Methods for computing the parameters

- Example of a sphere lit with a diffuse dome light:

	Wolff		
AOP φ	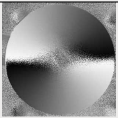		
DOP ρ	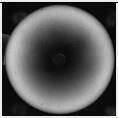		

[Wolff and Andreou, 1995]

Methods for computing the parameters

- Example of a sphere lit with a diffuse dome light:

	Wolff	Saito	
AOP φ	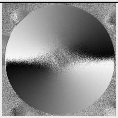	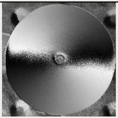	
DOP ρ	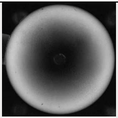	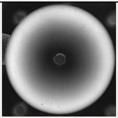	

[Wolff and Andreou, 1995] [Saito et al., 1999]

Methods for computing the parameters

- Example of a sphere lit with a diffuse dome light:

	Wolff	Saito	LMS
AOP φ	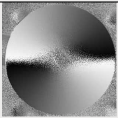	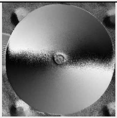	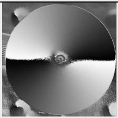
DOP ρ	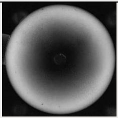	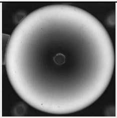	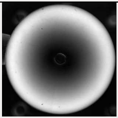

[Wolff and Andreou, 1995] [Saito et al., 1999]

Mueller calculus

Recall

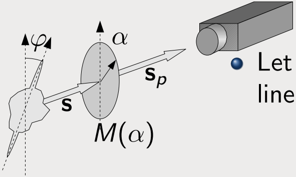

- Let be $M(\alpha)$ the mueller matrix of the linear polarizer:

$$M(\alpha) = \frac{1}{2}\begin{bmatrix} 1 & \cos 2\alpha & \sin 2\alpha & 0 \\ \cos 2\alpha & \cos^2 2\alpha & \cos 2\alpha \sin 2\alpha & 0 \\ \sin 2\alpha & \cos 2\alpha \sin 2\alpha & \sin^2 2\alpha & 0 \\ 0 & 0 & 0 & 0 \end{bmatrix}$$

Mueller calculus

Recall

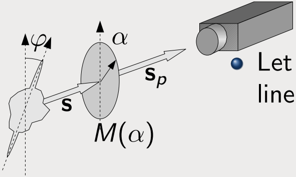

- Let be $M(\alpha)$ the mueller matrix of the linear polarizer:

$$M(\alpha) = \frac{1}{2}\begin{bmatrix} 1 & \cos 2\alpha & \sin 2\alpha & 0 \\ \cos 2\alpha & \cos^2 2\alpha & \cos 2\alpha \sin 2\alpha & 0 \\ \sin 2\alpha & \cos 2\alpha \sin 2\alpha & \sin^2 2\alpha & 0 \\ 0 & 0 & 0 & 0 \end{bmatrix}$$

$$\underbrace{\begin{bmatrix} s_{p_0} & s_{p_1} & s_{p_2} & s_{p_3} \end{bmatrix}^t}_{\mathbf{s_p}} = M(\alpha) \cdot \underbrace{\begin{bmatrix} s_0 & s_1 & s_2 & 0 \end{bmatrix}^t}_{\mathbf{s}}$$

Mueller calculus

Recall

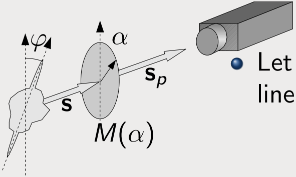

- Let be $M(\alpha)$ the mueller matrix of the linear polarizer:

$$M(\alpha) = \frac{1}{2}\begin{bmatrix} 1 & \cos 2\alpha & \sin 2\alpha & 0 \\ \cos 2\alpha & \cos^2 2\alpha & \cos 2\alpha \sin 2\alpha & 0 \\ \sin 2\alpha & \cos 2\alpha \sin 2\alpha & \sin^2 2\alpha & 0 \\ 0 & 0 & 0 & 0 \end{bmatrix}$$

$$\underbrace{\begin{bmatrix} s_{p_0} & s_{p_1} & s_{p_2} & s_{p_3} \end{bmatrix}^t}_{\mathbf{s_p}} = M(\alpha) \cdot \underbrace{\begin{bmatrix} s_0 & s_1 & s_2 & 0 \end{bmatrix}^t}_{\mathbf{s}}$$

- Since the sensor is only sensitive to light intensity $s_{p_0} = I_p$:

$$I_p = \frac{1}{2}\left(s_0 + s_1 \cos 2\alpha + s_2 \sin 2\alpha\right)$$

Least Mean Square method in details

Notations

- N images: $i = 1 \dots N$
- N values for the polarizer angle: $\alpha_1 \dots \alpha_2$
- $M = r \times c$ pixels: $j = 1 \dots M$

Least Mean Square method in details

Notations

- N images: $i = 1 \dots N$
- N values for the polarizer angle: $\alpha_1 \dots \alpha_2$
- $M = r \times c$ pixels: $j = 1 \dots M$

For every pixels: $j = 1 \dots M$

$$
\left| \begin{array}{ll}
P_1^j & = 0.5(s_0^j + s_1^j \cos 2\alpha_1 + s_2^j \sin 2\alpha_1) \\
P_2^j & = 0.5(s_0^j + s_1^j \cos 2\alpha_2 + s_2^j \sin 2\alpha_2) \\
\vdots & = \quad \vdots \\
P_N^j & = 0.5(s_0^j + s_1^j \cos 2\alpha_N + s_2^j \sin 2\alpha_N)
\end{array} \right.
$$

EndFor

Least Mean Square method in details

Notations

- N images: $i = 1 \dots N$
- N values for the polarizer angle: $\alpha_1 \dots \alpha_2$
- $M = r \times c$ pixels: $j = 1 \dots M$

For every pixels: $j = 1 \dots M$

$$\left| \begin{array}{ll} P_1^j & = 0.5(s_0^j + s_1^j \cos 2\alpha_1 + s_2^j \sin 2\alpha_1) \\ P_2^j & = 0.5(s_0^j + s_1^j \cos 2\alpha_2 + s_2^j \sin 2\alpha_2) \\ \vdots & = \quad \vdots \\ P_N^j & = 0.5(s_0^j + s_1^j \cos 2\alpha_N + s_2^j \sin 2\alpha_N) \end{array} \right.$$

EndFor

$$\underbrace{\begin{bmatrix} P_1^j \\ P_2^j \\ \vdots \\ P_N^j \end{bmatrix}}_{Y} = \frac{1}{2} \underbrace{\begin{bmatrix} 1 & \cos 2\alpha_1 & \sin 2\alpha_1 \\ 1 & \cos 2\alpha_2 & \sin 2\alpha_2 \\ \vdots & \vdots & \vdots \\ 1 & \cos 2\alpha_N & \sin 2\alpha_N \end{bmatrix}}_{A} \cdot \underbrace{\begin{bmatrix} s_0^j \\ s_1^j \\ s_2^j \end{bmatrix}}_{X}$$

Least Mean Square method in details

Notations

- N images: $i = 1 \dots N$
- N values for the polarizer angle: $\alpha_1 \dots \alpha_2$
- $M = r \times c$ pixels: $j = 1 \dots M$

For every pixels: $j = 1 \dots M$

$$
\begin{array}{|lll}
P_1^j & = 0.5(s_0^j + s_1^j \cos 2\alpha_1 + s_2^j \sin 2\alpha_1) \\
P_2^j & = 0.5(s_0^j + s_1^j \cos 2\alpha_2 + s_2^j \sin 2\alpha_2) \\
\vdots & = \quad \vdots \\
P_N^j & = 0.5(s_0^j + s_1^j \cos 2\alpha_N + s_2^j \sin 2\alpha_N)
\end{array}
$$

EndFor

$$
\underbrace{\begin{bmatrix} P_1^j \\ P_2^j \\ \vdots \\ P_N^j \end{bmatrix}}_{Y} = \frac{1}{2} \underbrace{\begin{bmatrix} 1 & \cos 2\alpha_1 & \sin 2\alpha_1 \\ 1 & \cos 2\alpha_2 & \sin 2\alpha_2 \\ \vdots & \vdots & \vdots \\ 1 & \cos 2\alpha_N & \sin 2\alpha_N \end{bmatrix}}_{A} \cdot \underbrace{\begin{bmatrix} s_0^j \\ s_1^j \\ s_2^j \end{bmatrix}}_{X}
$$

$$\Longrightarrow X = (A^t A)^{-1} A^t Y$$

An automatic optical device

By using a LCVR (Liquid Crystal Variable Retarder)

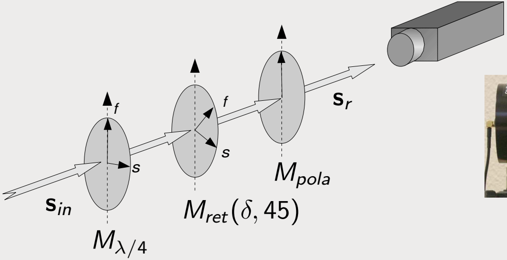

An automatic optical device

By using a LCVR (Liquid Crystal Variable Retarder)

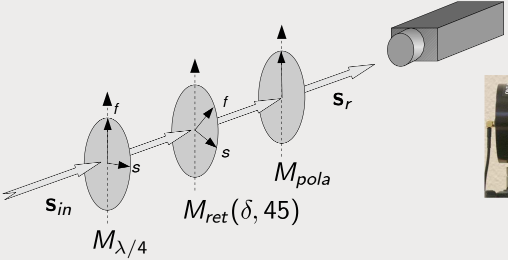

- Mueller calculus gives:

$$\mathbf{s}_r = M_{pola} \cdot M_{ret}(\delta, 45^\circ) \cdot M_{\lambda/4} \cdot \mathbf{s}_{in}$$

An automatic optical device

By using a LCVR (Liquid Crystal Variable Retarder)

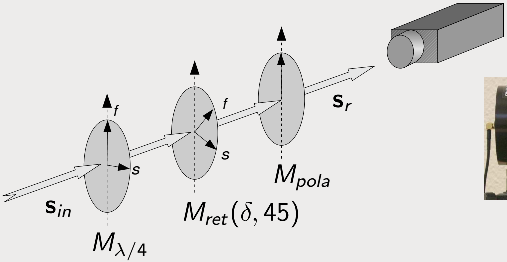

- Mueller calculus gives:

$$\mathbf{s}_r = M_{pola} \cdot M_{ret}(\delta, 45^\circ) \cdot M_{\lambda/4} \cdot \mathbf{s}_{in}$$

- Thus, the measured intensity I_r is:

$$I_r(\delta) = \frac{1}{2}(s_0 + s_1 \cos\delta + s_2 \sin\delta) = \frac{I}{2}(1 + \rho \cdot \cos(\delta - 2\varphi))$$

An automatic optical device

By using a LCVR (Liquid Crystal Variable Retarder)

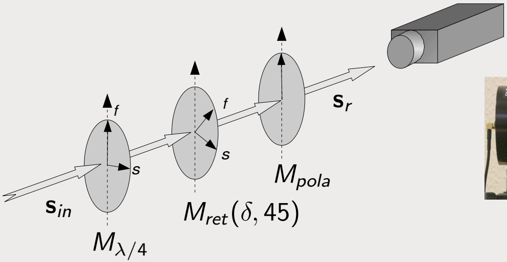

- Mueller calculus gives:

$$\mathbf{s}_r = M_{pola} \cdot M_{ret}(\delta, 45^\circ) \cdot M_{\lambda/4} \cdot \mathbf{s}_{in}$$

- Thus, the measured intensity I_r is:

$$I_r(\delta) = \frac{1}{2}(s_0 + s_1 \cos\delta + s_2 \sin\delta) = \frac{I}{2}(1 + \rho \cdot \cos(\delta - 2\varphi))$$

- by taking $\delta = 2\alpha \Longrightarrow$ this system is equivalent to the previous one

How to represent images of polarization parameters

Color representation

$$2\varphi \to H$$
$$I \to L$$
$$\rho \to L$$

[Wolff and Andreou, 1995]

How to represent images of polarization parameters

Color representation

$$2\varphi \rightarrow H$$
$$I \rightarrow L$$
$$\rho \rightarrow L$$

[Wolff and Andreou, 1995]

- Example:

How to represent images of polarization parameters

Color representation

$$2\varphi \rightarrow H$$
$$I \rightarrow L$$
$$\rho \rightarrow L$$

[Wolff and Andreou, 1995]

- Example:

How to represent images of polarization parameters

- Example: dielectric sphere lit by unpolarized light

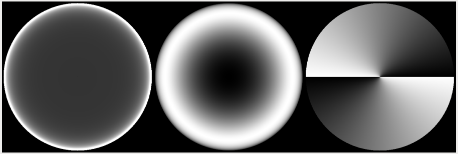

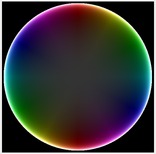

How to represent images of polarization parameters

- Example: dielectric sphere lit by unpolarized light

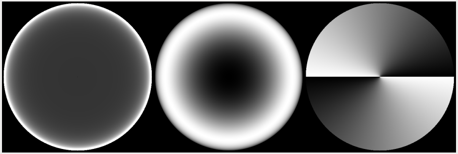

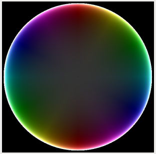

Other color representation

$$2\varphi \rightarrow H$$
$$I_{\|} + I_{\perp} \rightarrow L$$
$$I_{\|} - I_{\perp} \rightarrow S$$

[Tyo et al., 1998]

Outline

Stokes polarization imaging

Static set-up

- 2 steps process:

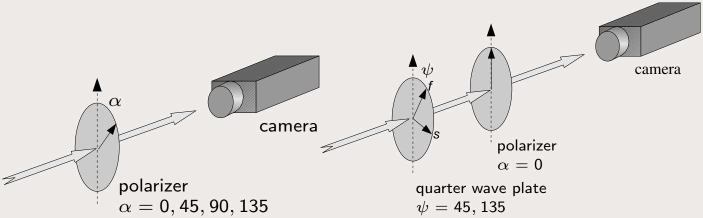

Stokes polarization imaging

Static set-up

- 2 steps process:

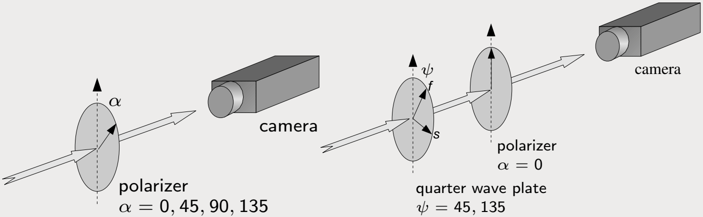

- Stokes vector computed for every pixels according to:

$$\begin{bmatrix} I_{0^\circ} + I_{90^\circ} \\ I_{0^\circ} - I_{90^\circ} \\ I_{45^\circ} - I_{135^\circ} \\ I_{45^\circ,\pi/2} - I_{135^\circ,\pi/2} \end{bmatrix}$$

Stokes polarization imaging

Dynamic set-up

- The process is fully automatic by using 2 LCVRs

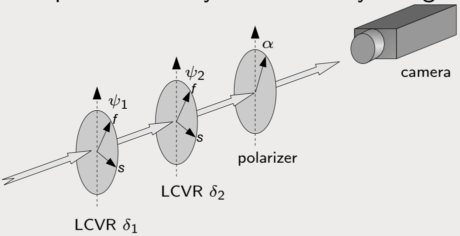

Mueller Computation

$$M_{dyn}(\delta_1,\,\delta_2) = M_{pola}(\alpha)\cdot M_{ret}(\delta_2,\,\psi_2)\cdot M_{ret}(\delta_1,\psi_1)$$

- α, ψ_1, ψ_2 are fixed. Several pairs of $(\delta_1,\,\delta_2)$ are used to estimate $[s_0, s_1, s_2, s_3]$ from:

$$I(\delta_1,\,\delta_2) = M_{dyn}^{11}s_0 + M_{dyn}^{12}s_1 + M_{dyn}^{13}s_2 + M_{dyn}^{14}s_3$$

Optimized pairs can be used to improve the SNR [Tyo, 2000, De Martino and Laude-Boulesteix, 2004]

Outline

Polarization cameras

Samba - Bossa Nova Tech

Specifications

- Polarization-difference imaging
- observed scene illuminated by a controlled source
- 10kHz polarization analysis

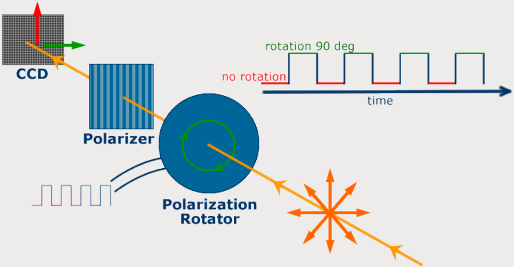

Polarization cameras

Salsa - Bossa Nova Tech

Specifications

- Full Stokes [Vedel et al., 2011]
- Ferroelectric crystals (FLC)
- 8 polarization frames/second

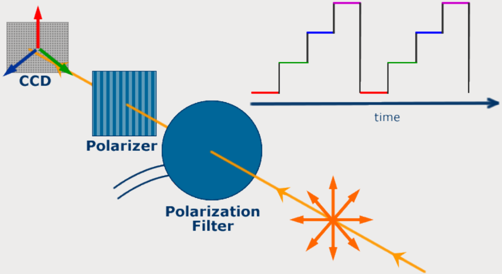

Polarization cameras

FluxData - Bossa Nova Tech

Specifications

- 3 different images
- No Ferroelectric crystal
- 30 polarization frames/second

Schematic View of 3-CCD Camera

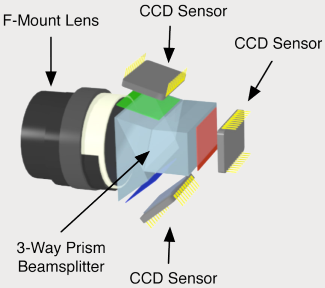

Outline

Unpolarized lightning

Physical principle

After being reflected, an unpolarized light wave becomes partially linearly polarized, depending on the surface normal and on the refractive index of the media it impinges on [Wolff and Boult, 1991].

Unpolarized lightning

Physical principle

After being reflected, an unpolarized light wave becomes partially linearly polarized, depending on the surface normal and on the refractive index of the media it impinges on [Wolff and Boult, 1991].

Polarization imaging system

- Simplified: if the three parameters are required
- Contrast ratio otherwise

Unpolarized lightning

Physical principle

After being reflected, an unpolarized light wave becomes partially linearly polarized, depending on the surface normal and on the refractive index of the media it impinges on [Wolff and Boult, 1991].

Polarization imaging system

- Simplified: if the three parameters are required
- Contrast ratio otherwise

Applications

- Vision through semi-reflecting media
- Material classification
- Separation of reflection components

Vision through semi-reflecting media

Purpose

Looking out a car (or room) window, one can see both the outside world (real object) and a semi-reflection of the objects inside (virtual objects).

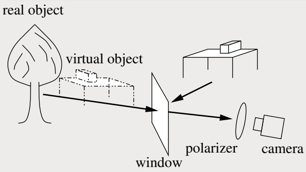

Vision through semi-reflecting media

Purpose

Looking out a car (or room) window, one can see both the outside world (real object) and a semi-reflection of the objects inside (virtual objects).

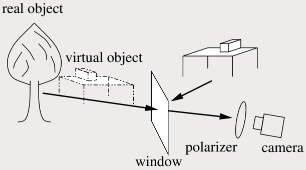

[Schechner et al., 2000]

Vision through semi-reflecting media

Example in Cairo 2009 - ICIP

Material classification

- The **diffuse component** of the reflected light is assumed to be unpolarized[Wolff and Boult, 1991]
- Expression of I_{max} and I_{min} seen through a rotating polarizer:

$$I_{max} = \frac{R_F}{R_F+1} I_s + \frac{1}{2} I_d, \quad I_{min} = \frac{1}{R_F+1} I_s + \frac{1}{2} I_d.$$

Material classification

- The **diffuse component** of the reflected light is assumed to be unpolarized[Wolff and Boult, 1991]
- Expression of I_{max} and I_{min} seen through a rotating polarizer:

$$I_{max} = \frac{R_F}{R_F + 1} I_s + \frac{1}{2} I_d, \quad I_{min} = \frac{1}{R_F + 1} I_s + \frac{1}{2} I_d.$$

$$I_{max} = R_F I_{min} + \frac{1 - R_F}{2} I_d$$

Material classification

- The **diffuse component** of the reflected light is assumed to be unpolarized[Wolff and Boult, 1991]
- Expression of I_{max} and I_{min} seen through a rotating polarizer:

$$I_{max} = \frac{R_F}{R_F + 1} I_s + \frac{1}{2} I_d, \quad I_{min} = \frac{1}{R_F + 1} I_s + \frac{1}{2} I_d.$$

$$I_{max} = R_F I_{min} + \frac{1 - R_F}{2} I_d$$

- Difficult in practice to estimate the Fresnel ratio R_F
- Dichromatic reflectance model [Nayar, 1997]
  - available for dielectrics (non-conductors)
  - the diffuse and specular components generally have different spectral distributions

Outline

Polarized lightning

Crossed polarization

- Frequently met in machine vision application
- Improvement of:
  - color constancy
  - image segmentation

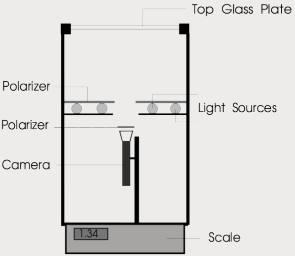

Polarized lightning

Crossed polarization

- Frequently met in machine vision application
- Improvement of:
  - color constancy
  - image segmentation

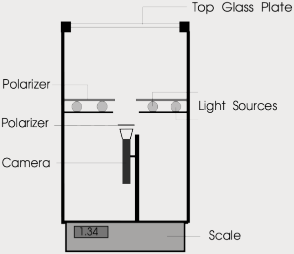

[Bolle et al., 1996]

Polarized lightning

Depolarization effect

Principle

A linearly polarized light wave reflected by a diffuse surface becomes unpolarized contrary to specular or metallic surfaces.

Polarized lightning

Depolarization effect

Principle

A linearly polarized light wave reflected by a diffuse surface becomes unpolarized contrary to specular or metallic surfaces.

- Discrimination on specular metallic surfaces between dust and surface defects:

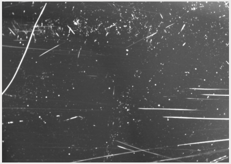

Parallel polarizer

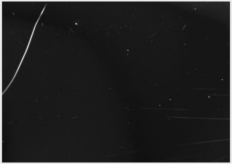

Crossed polarizer

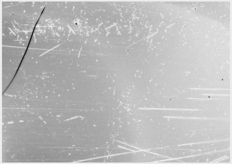

DOP

Polarized lightning

Depolarization effect in NIR

- A simplified Degree of Polarization is computed from 2 images according to:

$$D_p = \frac{I_{\parallel} - I_{\perp}}{I_{\parallel} + I_{\perp}}$$

Polarized lightning

Depolarization effect in NIR

- A simplified Degree of Polarization is computed from 2 images according to:

$$D_p = \frac{I_{\parallel} - I_{\perp}}{I_{\parallel} + I_{\perp}}$$

  - $D_p = 0 \Rightarrow$ depolarization effect (natural objects, lambertian surfaces)
  - $D_p = 1 \Rightarrow$ metallic surfaces, glass

Polarized lightning

Depolarization effect in NIR

- A simplified Degree of Polarization is computed from 2 images according to:

$$D_p = \frac{I_{\parallel} - I_{\perp}}{I_{\parallel} + I_{\perp}}$$

  - $D_p = 0 \Rightarrow$ depolarization effect (natural objects, lambertian surfaces)
  - $D_p = 1 \Rightarrow$ metallic surfaces, glass

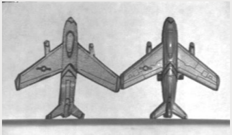

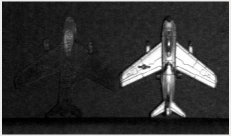

[Alouini et al., 2004]

Polarized lightning

Polarized light in Laser-scanning

Goal

Improving depth image acquisition by using polarized light to discriminate between primary and secondary reflection

Polarized lightning

Polarized light in Laser-scanning

Goal

Improving depth image acquisition by using polarized light to discriminate between primary and secondary reflection

- the laser line is linearly polarized
- an analyzer is placed in front of the sensor
- the polarization state of the reflected ray depends on both the incident angles and the number of interreflections
- [Clark et al., 1997, Wallace et al., 1999]

Polarized lightning

Material classification

Drawbacks of the Wolff method

- the angle of incidence is in the range 30-80 degree
- diffuse reflections must be negligible

Polarized lightning

Material classification

Drawbacks of the Wolff method

- the angle of incidence is in the range 30-80 degree
- diffuse reflections must be negligible

- [Chen and Wolff, 1998] have used a linearly polarized light source

Physical principles

When the linearly polarized light is reflected by a dielectric surface, it remains linearly polarized whereas it becomes ellipticaly polarized by a metallic surface

Polarized lightning

Material classification - polarization set-up

- Ellipticity of light has to be measured

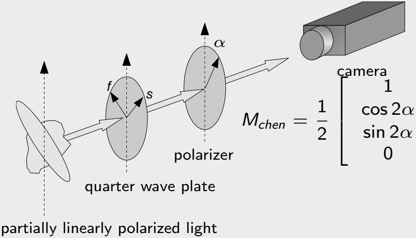

$$M_{chen} = \frac{1}{2}\begin{bmatrix} 1 & 0 & \sin 2\alpha & \cos 2\alpha \\ \cos 2\alpha & 0 & \cos 2\alpha \sin 2\alpha & \cos^2 2\alpha \\ \sin 2\alpha & 0 & \sin^2 2\alpha & \cos 2\alpha \sin 2\alpha \\ 0 & 0 & 0 & 0 \end{bmatrix}$$

Polarized lightning

Material classification - polarization set-up

- Ellipticity of light has to be measured

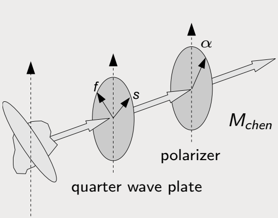

$$M_{chen} = \frac{1}{2}\begin{bmatrix} 1 & 0 & \sin 2\alpha & \cos 2\alpha \\ \cos 2\alpha & 0 & \cos 2\alpha \sin 2\alpha & \cos^2 2\alpha \\ \sin 2\alpha & 0 & \sin^2 2\alpha & \cos 2\alpha \sin 2\alpha \\ 0 & 0 & 0 & 0 \end{bmatrix}$$

- Intensity of measured light:

$$I_p = \frac{1}{2}(s_0 + s_2 \sin 2\alpha + s_3 \cos 2\alpha)$$

Polarized lightning

Material classification - polarization set-up

- Ellipticity of light has to be measured

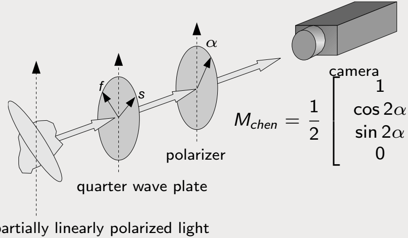

$$M_{chen} = \frac{1}{2}\begin{bmatrix} 1 & 0 & \sin 2\alpha & \cos 2\alpha \\ \cos 2\alpha & 0 & \cos 2\alpha \sin 2\alpha & \cos^2 2\alpha \\ \sin 2\alpha & 0 & \sin^2 2\alpha & \cos 2\alpha \sin 2\alpha \\ 0 & 0 & 0 & 0 \end{bmatrix}$$

- Intensity of measured light:

$$I_p = \frac{1}{2}(s_0 + s_2 \sin 2\alpha + s_3 \cos 2\alpha)$$

- Phase measurement:

$$\delta = \arctan s_3/s_2$$

Medical imagery

Polarimetric imaging for the diagnosis of cervical cancer

Diagnosis of Cervical cancer detection

- current strategy for the early detection and therapy:
  - Pap smear followed by a colposcopy if anomalous
- colposcopy is very difficult and operator-dependent $\Rightarrow$ significant proportion of wrong colposcopic diagnoses

Medical imagery

Polarimetric imaging for the diagnosis of cervical cancer

Diagnosis of Cervical cancer detection

- current strategy for the early detection and therapy:
  - Pap smear followed by a colposcopy if anomalous
- colposcopy is very difficult and operator-dependent $\Rightarrow$ significant proportion of wrong colposcopic diagnoses

[Anastasiadou et al., 2008]

- Polarization contrast measurement $\frac{I_{\parallel}-I_{\perp}}{I_{\parallel}+I_{\perp}}$

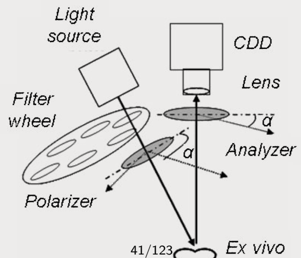

Medical imagery

Polarimetric imaging for the diagnosis of cervical cancer

- The precancerous lesions appearing less depolarizing

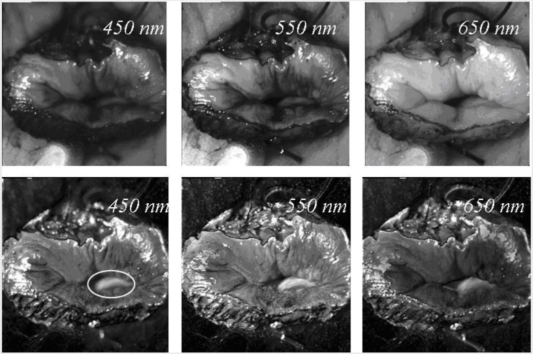

Imaging skin pathology

Principle

Propagation of light through a biological tissue causes changes due to tissue birefringence and scattering:

- light that propagates deeply escape with random polarization state
- on superficial tissue, polarization almost remains (region where cancer developps)

Imaging skin pathology

Principle

Propagation of light through a biological tissue causes changes due to tissue birefringence and scattering:

- light that propagates deeply escape with random polarization state
- on superficial tissue, polarization almost remains (region where cancer developps)

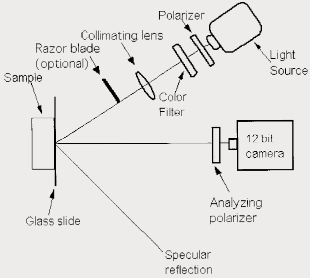

[Jacques et al., 2002]

Imaging skin pathology

- When the polarizer is parallal to the polarized light source

$$I_{\parallel} = I_0 T_{mel} \left(R_s + \frac{1}{2} R_d \right)$$

  - where T_{mel} is the absoprtion coefficient linked to the epidermal melanin effect
  - R_s is the superficially reflected light
  - R_d is the "deeply penetrating" light

Imaging skin pathology

- When the polarizer is parallal to the polarized light source

$$I_{\parallel} = I_0 T_{mel} \left(R_s + \frac{1}{2} R_d \right)$$

  - where T_{mel} is the absoprtion coefficient linked to the epidermal melanin effect
  - R_s is the superficially reflected light
  - R_d is the "deeply penetrating" light

- When the polarizer is perpendicular to the polarized source

$$I_{\perp} = I_0 T_{mel} \frac{1}{2} R_d$$

Imaging skin pathology

- When the polarizer is parallal to the polarized light source

$$I_{\parallel} = I_0 T_{mel} \left(R_s + \frac{1}{2} R_d \right)$$

  - where T_{mel} is the absoprtion coefficient linked to the epidermal melanin effect
  - R_s is the superficially reflected light
  - R_d is the "deeply penetrating" light

- When the polarizer is perpendicular to the polarized source

$$I_{\perp} = I_0 T_{mel} \frac{1}{2} R_d$$

- The polarization ratio is finally given by:

$$\frac{I_{\parallel} - I_{\perp}}{I_{\parallel} + I_{\perp}} = \frac{R_s}{R_s + R_d}$$

Imaging skin pathology

Results on normal skin

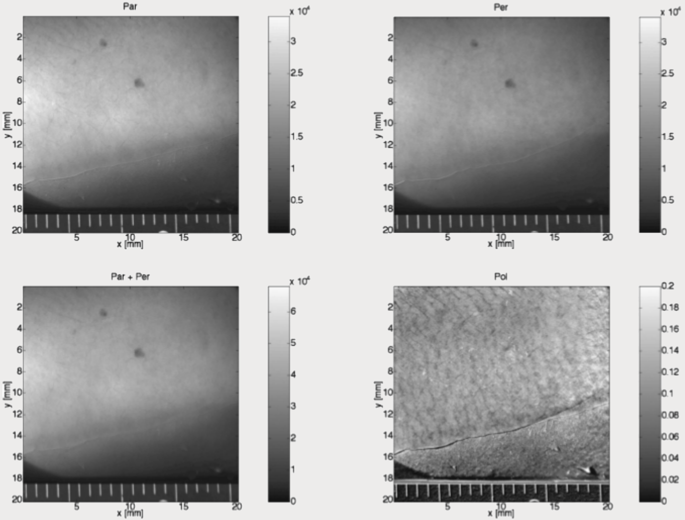

The strucural details of the superficial layer are emphasized.

Imaging skin pathology

Results on burn scar

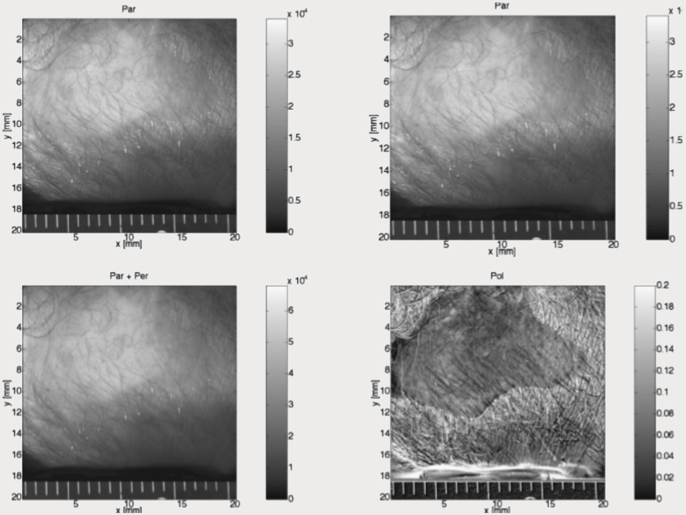

Imaging skin pathology

Results on carcinoma

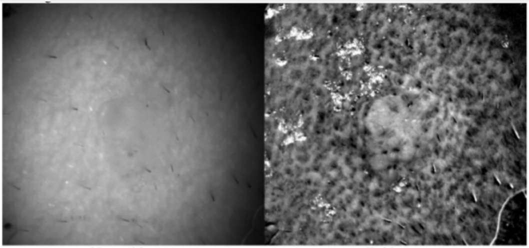

Malignant basal cell carcinoma

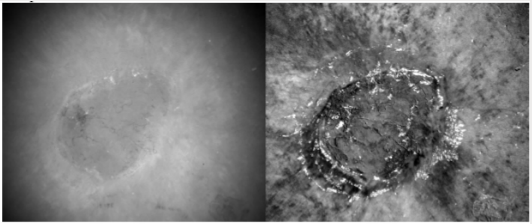

Squamous cell carcinoma

Outline

Introduction

Goal

The aim of Shape from Polarization is to provide the 3D shape of an object from polarization imaging.

Introduction

Goal

The aim of Shape from Polarization is to provide the 3D shape of an object from polarization imaging.

Main interests

Extract the 3D information of the surface from:

- Translucent objects
- Highly reflective objects

Introduction

Goal

The aim of Shape from Polarization is to provide the 3D shape of an object from polarization imaging.

Main interests

Extract the 3D information of the surface from:

- Translucent objects
- Highly reflective objects

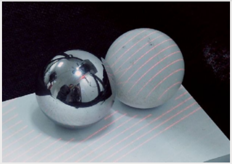

Introduction

Goal

The aim of Shape from Polarization is to provide the 3D shape of an object from polarization imaging.

Main interests

Extract the 3D information of the surface from:

- Translucent objects
- Highly reflective objects

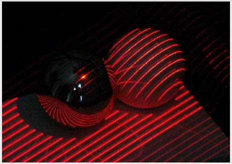

History

- **Koshikawa**: reflection of a circularly polarized wave to get the orientation of planar surfaces [Koshikawa, 1979]

History

- **Koshikawa**: reflection of a circularly polarized wave to get the orientation of planar surfaces [Koshikawa, 1979]
- **Wolff**: reflection of an unpolarized light [Wolff and Boult, 1991]
  - Reconstruction of dielectric surfaces:
    - [Miyazaki et al., 2004, Rahmann, 2003, Atkinson and Hancock, 2006]
  - Reconstruction of specular metallic surfaces
    - [Morel et al., 2006]

Physical principle

Used by Wolff and the rest

After being reflected, an unpolarized light wave becomes partially linearly polarized, depending on the surface normal and on the refractive index of the media it impinges on.

Physical principle

Used by Wolff and the rest

After being reflected, an unpolarized light wave becomes partially linearly polarized, depending on the surface normal and on the refractive index of the media it impinges on.

1. polarization parameters measurement
2. surface normals
3. height from gradients

Principle

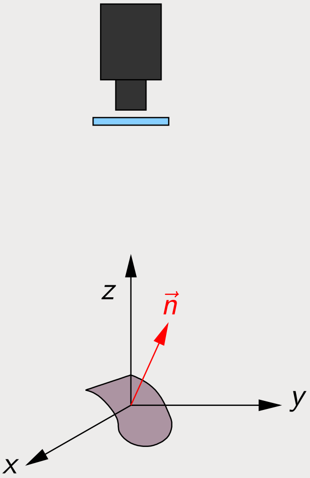

Required conditions

- Unpolarized lightning
- Highly reflective surface
- Telecentric lens

Principle

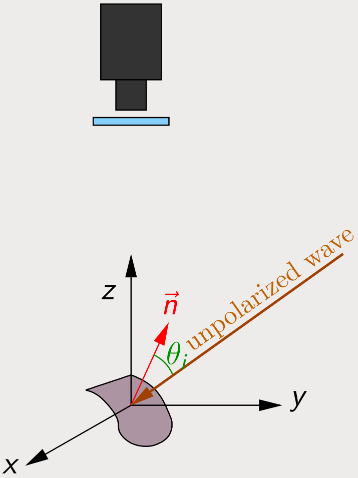

Required conditions

- Unpolarized lightning
- Highly reflective surface
- Telecentric lens

Principle

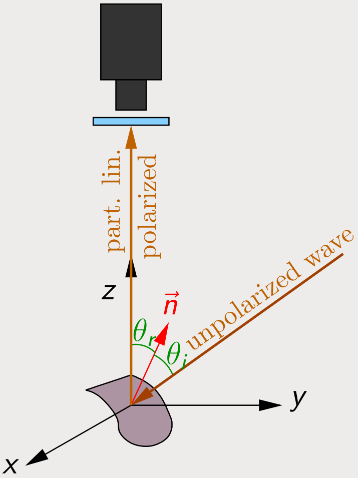

Required conditions

- Unpolarized lightning
- Highly reflective surface
- Telecentric lens

Principle

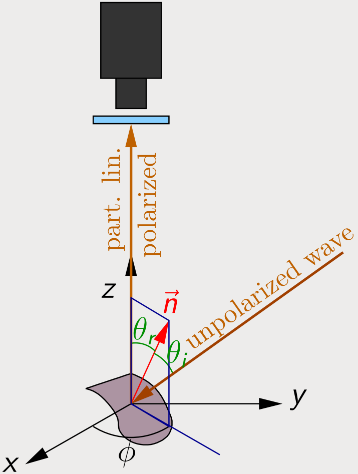

Required conditions

- Unpolarized lightning
- Highly reflective surface
- Telecentric lens

Principle

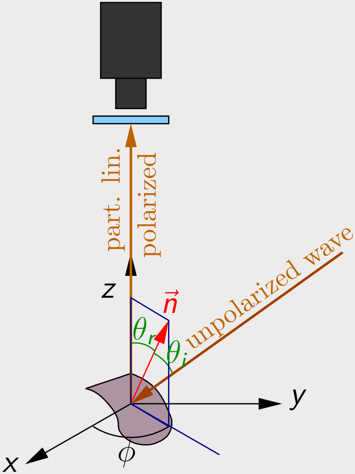

Required conditions

- Unpolarized lightning
- Highly reflective surface
- Telecentric lens

$$\vec{n} = \begin{pmatrix} p = \tan\theta_r \cos\phi \\ q = \tan\theta_r \sin\phi \\ 1 \end{pmatrix} \Rightarrow (\phi, \theta_r)\,?$$

Principle

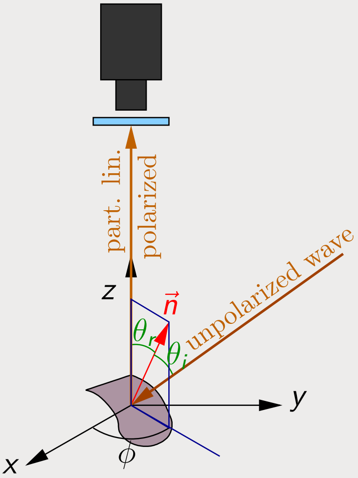

Required conditions

- Unpolarized lightning
- Highly reflective surface
- Telecentric lens

$$\vec{n} = \begin{pmatrix} p = \tan\theta_r \cos\phi \\ q = \tan\theta_r \sin\phi \\ 1 \end{pmatrix} \Rightarrow (\phi, \theta_r)\,?$$

Fresnel's coefficients:

- Angle of polarization: $\varphi \Rightarrow \phi$
- Degree of polarization: $\rho \Rightarrow \theta_r$

Recall of some basic optical laws

- Snell-Descartes' Law:

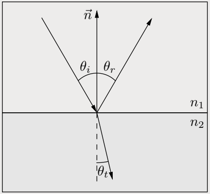

$$\begin{cases} \theta_i = \theta_r, \\ n_1 \sin\theta_i = n_2 \sin\theta_t. \end{cases}$$

Recall of some basic optical laws

- Snell-Descartes' Law:

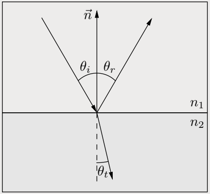

$$\begin{cases} \theta_i = \theta_r, \\ n_1 \sin\theta_i = n_2 \sin\theta_t. \end{cases}$$

- Fresnel formulae:

$$\begin{cases} f_\perp = \dfrac{R_\perp}{A_\perp} = -\dfrac{\sin(\theta_i - \theta_t)}{\sin(\theta_i + \theta_t)}, \\ f_\parallel = \dfrac{R_\parallel}{A_\parallel} = \dfrac{\tan(\theta_i - \theta_t)}{\tan(\theta_i + \theta_t)}. \end{cases}$$

Proof

By using the Mueller calculus once again

Mueller matrix of the specular reflection

The Mueller matrix of the specular reflection is given by the product of two matrices: Mueller matrix of a partial polarizer and the Mueller matrix of a perfect retarder.

$$M_{refl} = M_{pp}(F_\perp, F_\parallel) \cdot M_{ret}(\delta, 0)$$

with $F_\perp = |f_\perp|^2$, $F_\parallel = \left|f_\parallel\right|^2$ and $\delta = \arg(f_\parallel - f_\perp)$

Proof

By using the Mueller calculus once again

Mueller matrix of the specular reflection

The Mueller matrix of the specular reflection is given by the product of two matrices: Mueller matrix of a partial polarizer and the Mueller matrix of a perfect retarder.

$$M_{refl} = M_{pp}(F_\perp, F_\parallel) \cdot M_{ret}(\delta, 0)$$

with $F_\perp = |f_\perp|^2$, $F_\parallel = \left|f_\parallel\right|^2$ and $\delta = \arg(f_\parallel - f_\perp)$

$$M_{refl} = \frac{1}{2}\begin{bmatrix} F_\perp + F_\parallel & F_\perp - F_\parallel & 0 & 0 \\ F_\perp - F_\parallel & F_\perp + F_\parallel & 0 & 0 \\ 0 & 0 & 2\sqrt{F_\perp F_\parallel}\cos\delta & 2\sqrt{F_\perp F_\parallel}\sin\delta \\ 0 & 0 & -2\sqrt{F_\perp F_\parallel}\sin\delta & 2\sqrt{F_\perp F_\parallel}\cos\delta \end{bmatrix}$$

Reflection of an unpolarized light

- Incident light is assumed to be unpolarized:

$$\mathbf{s}^{(i)} = \begin{bmatrix} I_0 & 0 & 0 & 0 \end{bmatrix}^t$$

- The reflected light can be written:

$$\mathbf{s}^{(r)} = M_{refl} \cdot \mathbf{s}^{(i)} = \frac{I_0}{2} \begin{bmatrix} F_\perp + F_\parallel & F_\perp - F_\parallel & 0 & 0 \end{bmatrix}^t$$

Reflection of an unpolarized light

- Incident light is assumed to be unpolarized:

$$\mathbf{s}^{(i)} = \begin{bmatrix} I_0 & 0 & 0 & 0 \end{bmatrix}^t$$

- The reflected light can be written:

$$\mathbf{s}^{(r)} = M_{refl} \cdot \mathbf{s}^{(i)} = \frac{I_0}{2} \begin{bmatrix} F_\perp + F_\parallel & F_\perp - F_\parallel & 0 & 0 \end{bmatrix}^t$$

Conclusions

- the reflected light is partially polarized since: $s_0^2 \geq s_1^2 + 0 + 0$

Reflection of an unpolarized light

- Incident light is assumed to be unpolarized:

$$\mathbf{s}^{(i)} = \begin{bmatrix} I_0 & 0 & 0 & 0 \end{bmatrix}^t$$

- The reflected light can be written:

$$\mathbf{s}^{(r)} = M_{refl} \cdot \mathbf{s}^{(i)} = \frac{I_0}{2} \begin{bmatrix} F_\perp + F_\parallel & F_\perp - F_\parallel & 0 & 0 \end{bmatrix}^t$$

Conclusions

- the reflected light is partially polarized since: $s_0^2 \geq s_1^2 + 0 + 0$
- degree of polarization: $\rho = \frac{F_\perp - F_\parallel}{F_\perp + F_\parallel}$ $(F_\perp \geq F_\parallel)$

Reflection of an unpolarized light

- Incident light is assumed to be unpolarized:

$$\mathbf{s}^{(i)} = \begin{bmatrix} I_0 & 0 & 0 & 0 \end{bmatrix}^t$$

- The reflected light can be written:

$$\mathbf{s}^{(r)} = M_{refl} \cdot \mathbf{s}^{(i)} = \frac{I_0}{2} \begin{bmatrix} F_\perp + F_\parallel & F_\perp - F_\parallel & 0 & 0 \end{bmatrix}^t$$

Conclusions

- the reflected light is partially polarized since: $s_0^2 \geq s_1^2 + 0 + 0$
- degree of polarization: $\rho = \frac{F_\perp - F_\parallel}{F_\perp + F_\parallel}$ $(F_\perp \geq F_\parallel)$
- light intensity: $I = \frac{I_0}{2} \cdot (F_\perp + F_\parallel)$

Reflection of an unpolarized light

- Incident light is assumed to be unpolarized:

$$\mathbf{s}^{(i)} = \begin{bmatrix} I_0 & 0 & 0 & 0 \end{bmatrix}^t$$

- The reflected light can be written:

$$\mathbf{s}^{(r)} = M_{refl} \cdot \mathbf{s}^{(i)} = \frac{I_0}{2} \begin{bmatrix} F_\perp + F_\parallel & F_\perp - F_\parallel & 0 & 0 \end{bmatrix}^t$$

Conclusions

- the reflected light is partially polarized since: $s_0^2 \geq s_1^2 + 0 + 0$
- degree of polarization: $\rho = \frac{F_\perp - F_\parallel}{F_\perp + F_\parallel}$ $(F_\perp \geq F_\parallel)$
- light intensity: $I = \frac{I_0}{2} \cdot (F_\perp + F_\parallel)$
- ellipticity: $\chi = 0 \Rightarrow$ linearly polarized

Reflection of an unpolarized light

- Incident light is assumed to be unpolarized:

$$\mathbf{s}^{(i)} = \begin{bmatrix} I_0 & 0 & 0 & 0 \end{bmatrix}^t$$

- The reflected light can be written:

$$\mathbf{s}^{(r)} = M_{refl} \cdot \mathbf{s}^{(i)} = \frac{I_0}{2} \begin{bmatrix} F_\perp + F_\parallel & F_\perp - F_\parallel & 0 & 0 \end{bmatrix}^t$$

Conclusions

- the reflected light is partially polarized since: $s_0^2 \geq s_1^2 + 0 + 0$
- degree of polarization: $\rho = \frac{F_\perp - F_\parallel}{F_\perp + F_\parallel}$ $(F_\perp \geq F_\parallel)$
- light intensity: $I = \frac{I_0}{2} \cdot (F_\perp + F_\parallel)$
- ellipticity: $\chi = 0 \Rightarrow$ linearly polarized
- angle of polarization: $\varphi = 0 \Rightarrow$ the linearly polarized component is orthogonal to the plane of incidence

Outline

Degree of polarization $\rho \Rightarrow \theta_r$

Degree of polarization

$$\rho = \frac{F_\perp - F_\parallel}{F_\perp + F_\parallel}$$

- From the Fresnel formulae, we know that $F_\perp$ and $F_\parallel$ depend of θ_i and θ_t

Degree of polarization $\rho \Rightarrow \theta_r$

Degree of polarization

$$\rho = \frac{F_\perp - F_\parallel}{F_\perp + F_\parallel}$$

- From the Fresnel formulae, we know that $F_\perp$ and $F_\parallel$ depend of θ_i and θ_t
- And from the Snell-Descartes' law, one can write:

$$\theta_t = \arcsin\left(\frac{1}{n}\sin\theta_i\right)$$

Degree of polarization $\rho \Rightarrow \theta_r$

Degree of polarization

$$\rho = \frac{F_\perp - F_\parallel}{F_\perp + F_\parallel}$$

- From the Fresnel formulae, we know that $F_\perp$ and $F_\parallel$ depend of θ_i and θ_t
- And from the Snell-Descartes' law, one can write:

$$\theta_t = \arcsin\left(\frac{1}{n}\sin\theta_i\right)$$

- Therefore, since $\theta_i = \theta_r$ we can deduce that $F_\perp$ and $F_\parallel$ depend of θ_r and n

Degree of polarization $\rho \Rightarrow \theta_r$

Degree of polarization

$$\rho = \frac{F_\perp - F_\parallel}{F_\perp + F_\parallel}$$

- From the Fresnel formulae, we know that $F_\perp$ and $F_\parallel$ depend of θ_i and θ_t
- And from the Snell-Descartes' law, one can write:

$$\theta_t = \arcsin\left(\frac{1}{n}\sin\theta_i\right)$$

- Therefore, since $\theta_i = \theta_r$ we can deduce that $F_\perp$ and $F_\parallel$ depend of θ_r and n
- If the object refractive index n is known we have $\rho(\theta_r)$

Degree of polarization $\rho \Rightarrow \theta_r$

For dielectric surfaces:

$$\rho = \frac{2\sin^2\theta\sqrt{n^2 - \sin^2\theta - n^2\sin^2\theta + \sin^4\theta}}{n^2 - \sin^2\theta - n^2\sin^2\theta + 2\sin^4\theta}$$

Degree of polarization $\rho \Rightarrow \theta_r$

For dielectric surfaces:

$$\rho = \frac{2\sin^2\theta\sqrt{n^2 - \sin^2\theta - n^2\sin^2\theta + \sin^4\theta}}{n^2 - \sin^2\theta - n^2\sin^2\theta + 2\sin^4\theta}$$

For metallic surfaces

$$\rho(\theta) = \frac{2n\tan\theta\sin\theta}{\tan^2\theta\sin^2\theta + |\hat{n}|^2},$$

where $\hat{n}$ is the complex refractive index and according the approximation $|\hat{n}|^2 = n^2(1+\kappa^2) \gg 1$[Born and Wolf, 1999]

Relationship between ρ and θ for dielectric surfaces

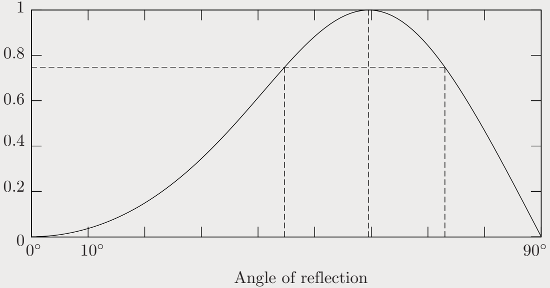

Relationship between ρ and θ for dielectric surfaces

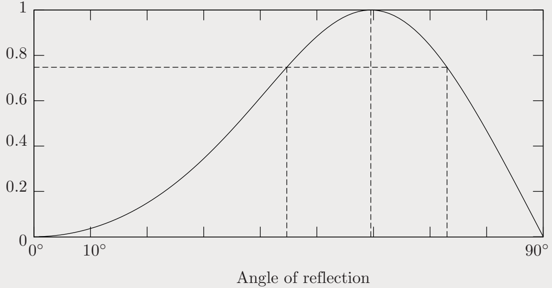

- Ambiguity problem to be solved
  - with two images [Miyazaki et al., 2004]: normal position and tilted with small angle position
  - with thermal imagery [Miyazaki et al., 2002]

Disambiguation by thermal imagery

[Miyazaki et al., 2002]

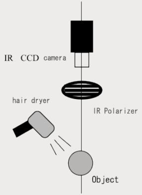

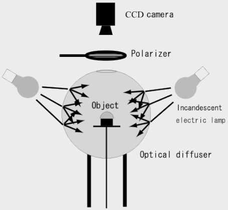

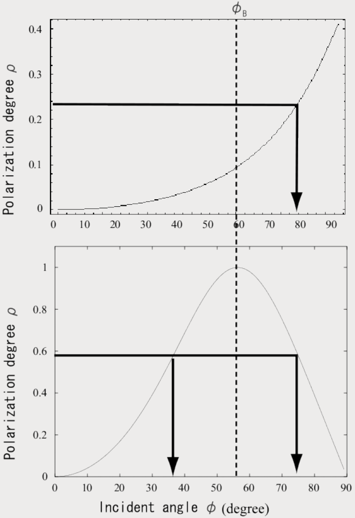

Relationship between ρ and θ for metallic surfaces

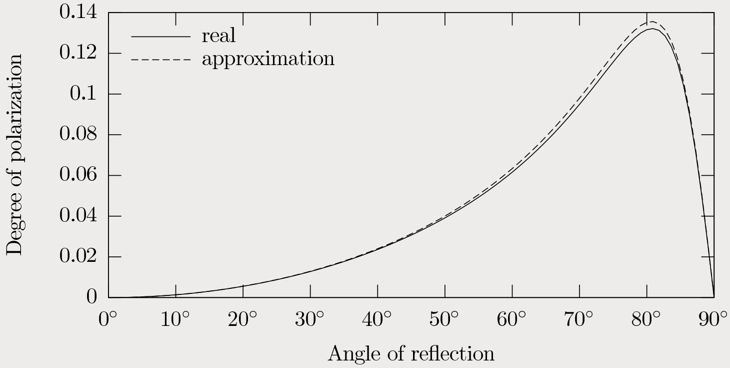

Relationship between ρ and θ for metallic surfaces

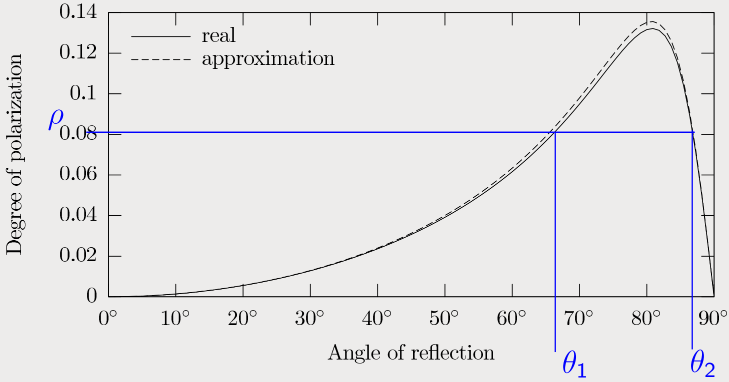

Relationship between ρ and θ for metallic surfaces

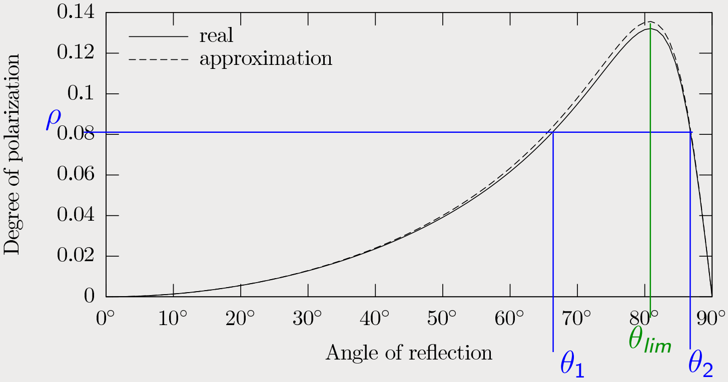

- θ_{lim} : principal angle of incidence
- $\theta_{lim} \simeq 80°$

Angle of polarization $\varphi \Rightarrow \phi$

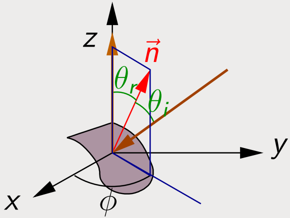

Property

The reflected light is partially linearly polarized orthogonally to the plane of incidence.

$$\phi = \varphi \pm \frac{\pi}{2}$$

Angle of polarization $\varphi \Rightarrow \phi$

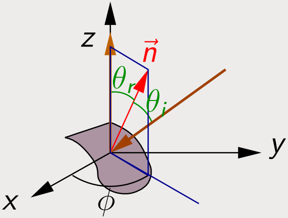

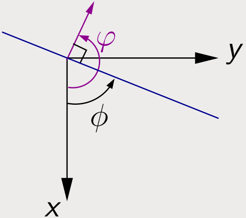

Property

The reflected light is partially linearly polarized orthogonally to the plane of incidence.

$$\phi = \varphi \pm \frac{\pi}{2}$$

Angle of polarization $\varphi \Rightarrow \phi$

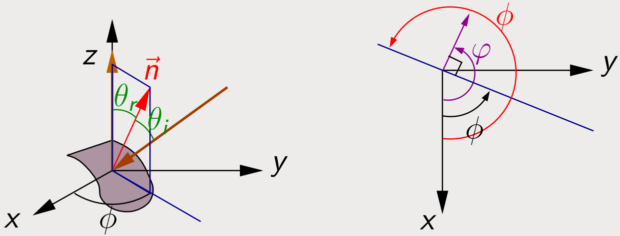

Property

The reflected light is partially linearly polarized orthogonally to the plane of incidence.

$$\phi = \varphi \pm \frac{\pi}{2}$$

$\Rightarrow$ ambiguity in the determination of ϕ

Solving the ambiguity

By using ϕ at the occluding boundary [Miyazaki et al., 2004]

- object must be closed
- the normal has to be computed at the occluding boundary
- this initial condition has to be propagated throughout the surface
- it assumes that all local parts of the surface are not concave toward the camera direction.

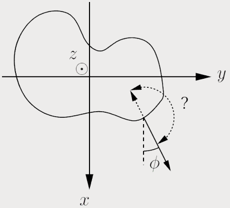

Active lighting

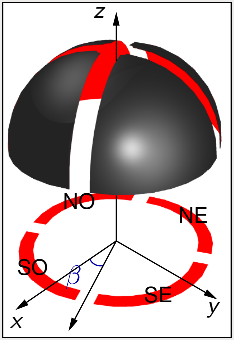

$\beta \in]0, \pi/2[$

Active lighting

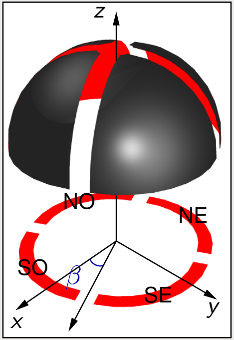

$\beta \in]0, \pi/2[$

- E/W Segmentation

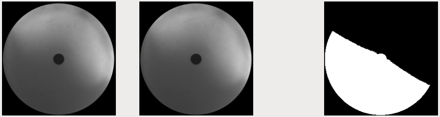

Active lighting

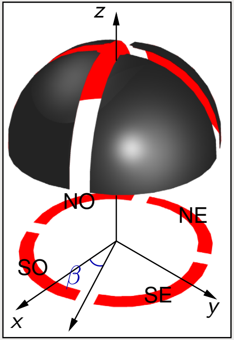

$\beta \in]0, \pi/2[$

- E/W Segmentation

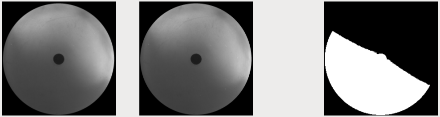

- N/S Segmentation

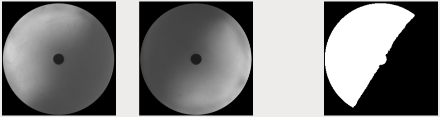

Active lighting

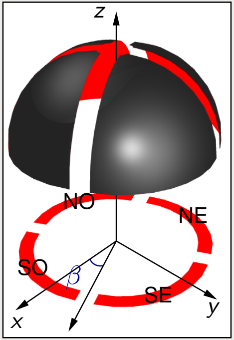

$\beta \in]0, \pi/2[$

- E/W Segmentation

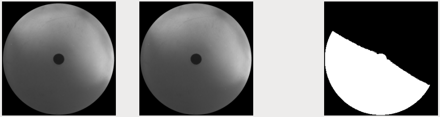

- N/S Segmentation

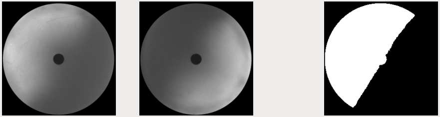

- Segmented image I_{quad}

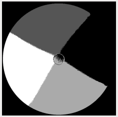

Active lighting

1. $\phi = \varphi - \pi/2$

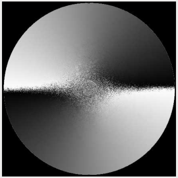

$\phi \in [\pi]$

Active lighting

1. $\phi = \varphi - \pi/2$

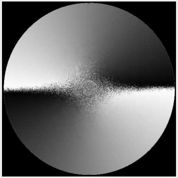

$\phi \in [\pi]$

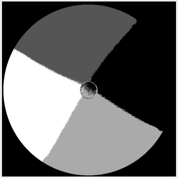

I_{quad}

2. $\phi = \phi + \pi$, if :

- $I_{quad} = 1$
- $(I_{quad} = 3) \wedge (\phi \geq 0)$
- $(I_{quad} = 0) \wedge (\phi \leq 0)$

Active lighting

1. $\phi = \varphi - \pi/2$

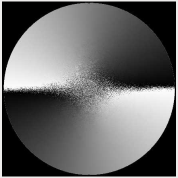

$\phi \in [\pi]$

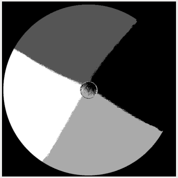

I_{quad}

2. $\phi = \phi + \pi$, if :
   - $I_{quad} = 1$
   - $(I_{quad} = 3) \wedge (\phi \geq 0)$
   - $(I_{quad} = 0) \wedge (\phi \leq 0)$

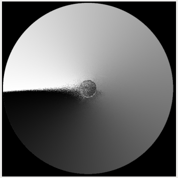

$\phi \in [2\pi]$

Active lighting

1. $\phi = \varphi - \pi/2$

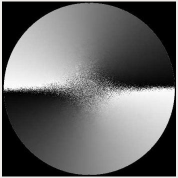

$\phi \in [\pi]$

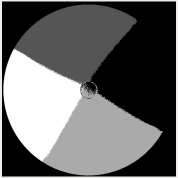

I_{quad}

2. $\phi = \phi + \pi$, if :
   - $I_{quad} = 1$
   - $(I_{quad} = 3) \wedge (\phi \geq 0)$
   - $(I_{quad} = 0) \wedge (\phi \leq 0)$

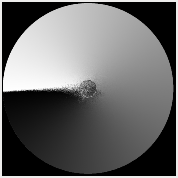

$\phi \in [2\pi]$

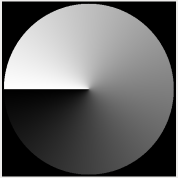

theoretical value of ϕ

Outline

Principle

Constraints

- Smooth surface, describe by a continuous function f, of C^2 class
- The height z can be written: $$f : \begin{array}{l} U \to \mathbb{R} \\ (x,y) \mapsto z = f(x,y) \end{array}$$

Principle

Constraints

- Smooth surface, describe by a continuous function f, of C^2 class
- The height z can be written: $\begin{aligned} f: \quad & U \to \mathbb{R} \\ & (x, y) \mapsto z = f(x, y) \end{aligned}$

Expression of the normal $\vec{n}$ for every points (x, y, z) of the surface:

$$\vec{n} = \begin{pmatrix} p = \tan\theta\cos\phi \\ q = \tan\theta\sin\phi \\ 1 \end{pmatrix}$$

Principle

Constraints

- Smooth surface, describe by a continuous function f, of C^2 class
- The height z can be written: $\begin{array}{ll} f: & U \to \mathbb{R} \\ & (x,y) \mapsto z = f(x,y) \end{array}$

Expression of the normal $\vec{n}$ for every points (x, y, z) of the surface:

$$\vec{n} = \begin{pmatrix} p = \tan\theta\cos\phi \\ q = \tan\theta\sin\phi \\ 1 \end{pmatrix} = \begin{pmatrix} -\frac{\partial f(x,y)}{\partial x} \\ -\frac{\partial f(x,y)}{\partial y} \\ 1 \end{pmatrix}$$

Principle

Example in 1D

- Example in 1D
    - Continuous representation of the derivative: $p(x) = -\frac{df(x)}{dx}$
    - Discrete approximation of the derivative: $p_i = -\frac{z_i - z_{i-1}}{\epsilon}$

Principle

Example in 1D

- Example in 1D
  - Continuous representation of the derivative: $p(x) = -\frac{df(x)}{dx}$
  - Discrete approximation of the derivative: $p_i = -\frac{z_i - z_{i-1}}{\epsilon}$
  - Integration process: $z_i = z_{i-1} - \epsilon p_i$
    - cumulative sum along a path
    - z is obtained up to a constant

Principle

Example in 1D

- Example in 1D
  - Continuous representation of the derivative: $p(x) = -\frac{df(x)}{dx}$
  - Discrete approximation of the derivative: $p_i = -\frac{z_i - z_{i-1}}{\epsilon}$
  - Integration process: $z_i = z_{i-1} - \epsilon p_i$
    - cumulative sum along a path
    - z is obtained up to a constant
- From 2 gradient images compute 1 surface...

Local methods

Rectangular integration

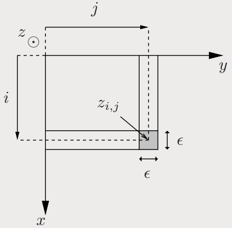

Local methods

Rectangular integration

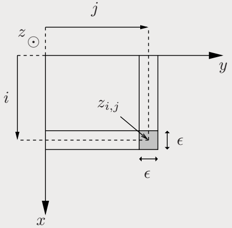

- For a **rectangular** integration, we get:

$$\begin{cases} z_{i,j} = z_{i-1,j} - \epsilon \cdot p_{i-1,j} \\ z_{i,j} = z_{i,,j-1} - \epsilon \cdot q_{i,j-1} \end{cases}$$

Local rectangular integration

$$z_{i,j} = \frac{z_{i-1,j} + z_{i,j-1}}{2} - \epsilon \frac{p_{i-1,j} + q_{i,j-1}}{2}$$

Local methods

Trapezoidal integration

- For a **trapezoidal** integration, we get:

$$\begin{cases} z_{i,j} = z_{i-1,j} - \epsilon \cdot p_{i-1,j} - \frac{\epsilon^2}{2} \cdot p'_{i-1,j} \\ z_{i,j} = z_{i,j-1} - \epsilon \cdot q_{i,j-1} - \frac{\epsilon^2}{2} \cdot q'_{i,j-1} \end{cases}$$

- p' and q' can be determined by:

$$\begin{cases} p'_{i-1,j} = \frac{p_{i,j} - p_{i-1,j}}{\epsilon} \\ q'_{i,j-1} = \frac{q_{i,j} - q_{i,j-1}}{\epsilon} \end{cases}$$

Local methods

Trapezoidal integration

- For a **trapezoidal** integration, we get:

$$\begin{cases} z_{i,j} = z_{i-1,j} - \epsilon \cdot p_{i-1,j} - \frac{\epsilon^2}{2} \cdot p'_{i-1,j} \\ z_{i,j} = z_{i,j-1} - \epsilon \cdot q_{i,j-1} - \frac{\epsilon^2}{2} \cdot q'_{i,j-1} \end{cases}$$

- p' and q' can be determined by:

$$\begin{cases} p'_{i-1,j} = \frac{p_{i,j} - p_{i-1,j}}{\epsilon} \\ q'_{i,j-1} = \frac{q_{i,j} - q_{i,j-1}}{\epsilon} \end{cases}$$

Local trapezoidal inegration

$$z_{i,j} = \frac{z_{i-1,j} + z_{i,j-1}}{2} - \epsilon \frac{p_{i,j} + p_{i-1,j} + q_{i,j} + q_{i,j-1}}{4}$$

Local methods

Ben Slimane

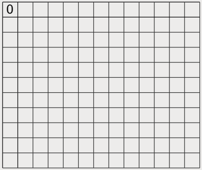

Local methods

Ben Slimane

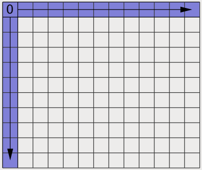

Local methods

Ben Slimane

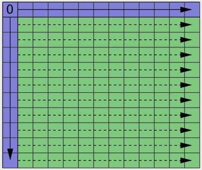

Local methods

Ben Slimane

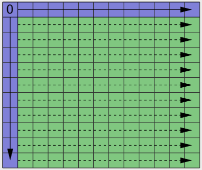

Coleman-Jain

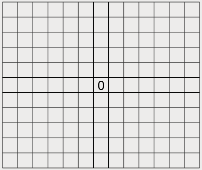

Local methods

Ben Slimane

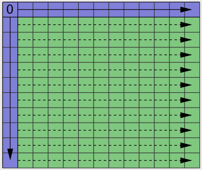

Coleman-Jain

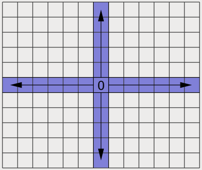

Local methods

Ben Slimane

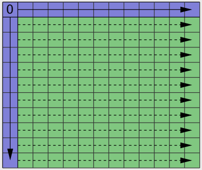

Coleman-Jain

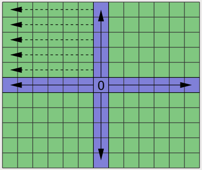

Local methods

Ben Slimane

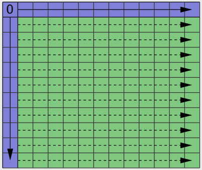

Coleman-Jain

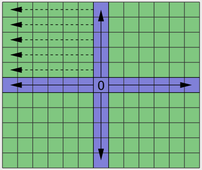

Rodehorst

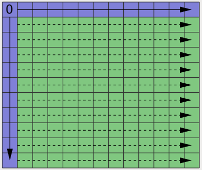

Local methods

Ben Slimane

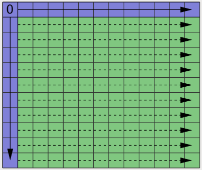

Coleman-Jain

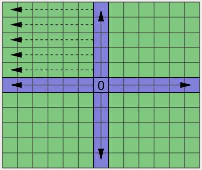

Rodehorst

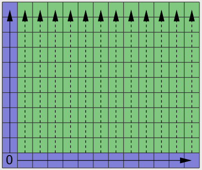

Local methods

Ben Slimane

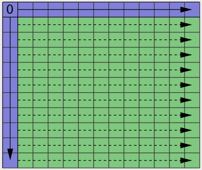

Coleman-Jain

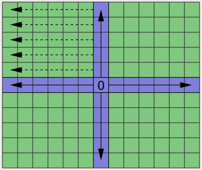

Rodehorst

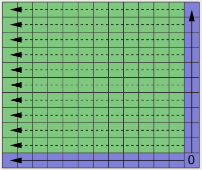

Local methods

Ben Slimane

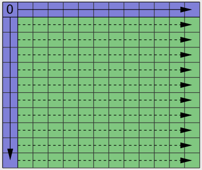

Coleman-Jain

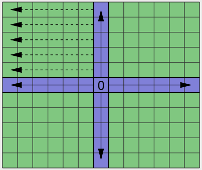

Rodehorst

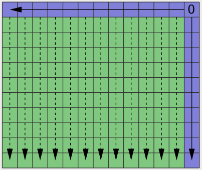

Local methods

Ben Slimane

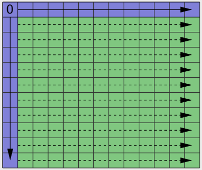

Coleman-Jain

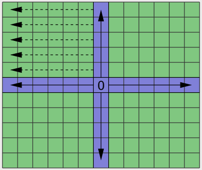

Rodehorst

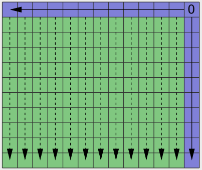

Reconstruction error of a gradient field computed from a plane $z = 0$

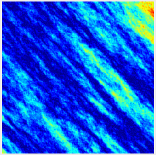

MSE=0.0477

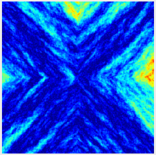

MSE=0.0444

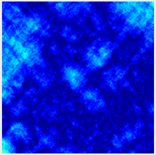

MSE=0.0273

Methods based on relaxation

Principle

Integration of the surface by minimizing the functional:

$$W = \int\int \left(\left(-\frac{\partial f(x,y)}{\partial x}\right) - p\right)^2 + \left(\left(-\frac{\partial f(x,y)}{\partial y}\right) - q\right)^2 dxdy$$

Methods based on relaxation

Principle

Integration of the surface by minimizing the functional:

$$W = \int\int \left(\left(-\frac{\partial f(x,y)}{\partial x}\right) - p\right)^2 + \left(\left(-\frac{\partial f(x,y)}{\partial y}\right) - q\right)^2 dxdy$$

- Comes from "Shape from Shading" algorithms [Ikeuchi, 1983, Horn and Brooks, 1986]

Methods based on relaxation

Principle

Integration of the surface by minimizing the functional:

$$W = \int\int \left(\left(-\frac{\partial f(x,y)}{\partial x}\right) - p\right)^2 + \left(\left(-\frac{\partial f(x,y)}{\partial y}\right) - q\right)^2 dxdy$$

- Comes from "Shape from Shading" algorithms [Ikeuchi, 1983, Horn and Brooks, 1986]

Iterative scheme

$$f(x,y)^{n+1} = \bar{f}(x,y)^n - \rho\left(\frac{\partial p}{\partial x} + \frac{\partial q}{\partial y}\right)$$

Methods based on relaxation

- Jacobi

$$\begin{aligned} z_{i,j}^{n+1} &= \frac{1}{4}\left(z_{i-1,j}^{n} + z_{i+1,j}^{n} + z_{i,j-1}^{n} + z_{i,j+1}^{n}\right) \\ &\quad -\frac{\epsilon}{4}\left(p_{i+1,j} - p_{i,j} + q_{i,j+1} - q_{i,j}\right) \end{aligned}$$

Methods based on relaxation

- Jacobi
- Gauss-Seidel

$$z_{i,j}^{n+1} = \frac{1}{4}\left(z_{i-1,j}^{n+1} + z_{i+1,j}^{n} + z_{i,j-1}^{n+1} + z_{i,j+1}^{n}\right) - \frac{\epsilon}{4}(p_{i+1,j} - p_{i,j} + q_{i,j+1} - q_{i,j})$$

$\Rightarrow$ the average is done on the most recent data

Methods based on relaxation

- Jacobi
- Gauss-Seidel
- SOR

$$
\begin{aligned}
z_{i,j}^{n+1} &= (1-\omega) z_{i,j}^{n} + \frac{\omega}{4}\left(z_{i-1,j}^{n+1} + z_{i+1,j}^{n} + z_{i,j-1}^{n+1} + z_{i,j+1}^{n}\right) \\
&\quad - \frac{\omega\epsilon}{4}\left(p_{i+1,j} - p_{i,j} + q_{i,j+1} - q_{i,j}\right)
\end{aligned}
$$

$\Rightarrow$ where ω is an "over relaxation" parameter: $1 < \omega < 2$

Methods based on relaxation

- Jacobi
- Gauss-Seidel
- SOR
- Generalization on a higher neighborhood

$$z_{i,j}^{n+1} = (1-\omega) z_{i,j}^{n} + \frac{\omega}{S} H \tilde{*} z_{i,j}^{n} - \frac{\omega a \epsilon}{2S} (p_{i+1,j} - p_{i,j} + q_{i,j+1} - q_{i,j})$$

$\Rightarrow$ where H is a symmetric averaging filter, S is the sum of the filter coefficients and a is a constant given by:

$$a = \sum_u \sum_v H(u,v) u^2 = \sum_u \sum_v H(u,v) v^2$$

Methods based on relaxation

- Jacobi
- Gauss-Seidel
- SOR
- Generalization on a higher neighborhood

Example:

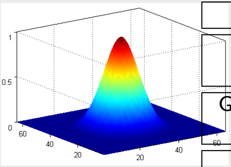

$MSE \leq 0.001$

method	neighborhood	nb of iterations	time(s
Jacobi	4	6475	11.64
	8	3374	3.67
Gauss-Seidel	4	890	1.01
	8	592	0.87
SOR	4	43	0.047
	8	42	0.045

Global methods

Basis projections

[Kovesi, 2003]

Correlation between the gradient and the gradients of basis functions gradients $\Leftrightarrow$ direct correlation between the surface and the basis functions.

- Robust method
- Reconstruction up to a scale factor

Global methods

Basis projections

[Kovesi, 2003]

Correlation between the gradient and the gradients of basis functions gradients $\Leftrightarrow$ direct correlation between the surface and the basis functions.

- Robust method
- Reconstruction up to a scale factor

[Karaçali and Snyder, 2003]

Projection of the surface gradients on a subset of gradient field.

- Reconstruction by part
- Very very time consuming

Global methods

Fourier transform

Principle

Minimizing the functional:

$$W = \int\int\left(\left(-\frac{\partial f(x,y)}{\partial x}\right) - p\right)^2 + \left(\left(-\frac{\partial f(x,y)}{\partial y}\right) - q\right)^2 dxdy$$

Global methods

Fourier transform

Principle

Minimizing the functional:

$$W = \int\int \left(\left(-\frac{\partial f(x,y)}{\partial x}\right) - p\right)^2 + \left(\left(-\frac{\partial f(x,y)}{\partial y}\right) - q\right)^2 dxdy$$

- Fourier transform of the surface:

$$\tilde{f}(u,v) = \int\int f(u,v) e^{-j(ux+vy)} dxdy$$

- The Parseval theorem:

$$\int\int |h(x,y)|^2 \, dxdy = \frac{1}{2\pi} \int\int \left|\tilde{h}(u,v)\right|^2 dudv$$

Global methods

Fourier transform

Principle

Minimizing the functional:

$$W = \int\int \left(\left(-\frac{\partial f(x,y)}{\partial x}\right) - p\right)^2 + \left(\left(-\frac{\partial f(x,y)}{\partial y}\right) - q\right)^2 dxdy$$

- Fourier transform of the surface:

$$\tilde{f}(u,v) = \int\int f(u,v)e^{-j(ux+vy)}dxdy$$

- The Parseval theorem:

$$\int\int |h(x,y)|^2 dxdy = \frac{1}{2\pi}\int\int \left|\tilde{h}(u,v)\right|^2 dudv$$

- Parseval theorem applied to the functional:

$$W = \frac{1}{2\pi}\int\int \left|-ju\tilde{f}(u,v) - \tilde{p}\right|^2 + \left|-jv\tilde{f}(u,v) - \tilde{q}\right|^2 dudv$$

Global methods

Fourier transform

- By expanding we get:

$$W = \frac{1}{2\pi}\int\int (u^2+v^2)\tilde{f}\tilde{f}^* + ju\tilde{p}^*\tilde{f} - ju\tilde{p}\tilde{f}^* + jv\tilde{q}^*\tilde{f} - jv\tilde{q}\tilde{f}^* + \tilde{p}\tilde{p}^* + \tilde{q}\tilde{q}^*\, dudv$$

where $\tilde{p}$ and $\tilde{q}$ are the Fourier transforms of the gradient.

Global methods

Fourier transform

- By expanding we get:

$$W = \frac{1}{2\pi}\int\int (u^2+v^2)\tilde{f}\tilde{f}^* + ju\tilde{p}^*\tilde{f} - ju\tilde{p}\tilde{f}^* + jv\tilde{q}^*\tilde{f} - jv\tilde{q}\tilde{f}^* + \tilde{p}\tilde{p}^* + \tilde{q}\tilde{q}^*\, dudv$$

where $\tilde{p}$ and $\tilde{q}$ are the Fourier transforms of the gradient.

- Differentiating the above expression with respect to $\tilde{f}$ and $\tilde{f}^*$ we can deduce the minimal conditions for the cost function:

$$\begin{cases} (u^2+v^2)\tilde{f}^* + ju\tilde{p}^* + jv\tilde{q}^* = 0, \\ (u^2+v^2)\tilde{f} - ju\tilde{p} - jv\tilde{q} = 0. \end{cases}$$

Global methods

Fourier transform

- By expanding we get:

$$W = \frac{1}{2\pi}\int\int (u^2+v^2)\tilde{f}\tilde{f}^* + ju\tilde{p}^*\tilde{f} - ju\tilde{p}\tilde{f}^* + jv\tilde{q}^*\tilde{f} - jv\tilde{q}\tilde{f}^* + \tilde{p}\tilde{p}^* + \tilde{q}\tilde{q}^*\, dudv$$

where $\tilde{p}$ and $\tilde{q}$ are the Fourier transforms of the gradient.

- Differentiating the above expression with respect to $\tilde{f}$ and $\tilde{f}^*$ we can deduce the minimal conditions for the cost function:

$$\begin{cases} (u^2+v^2)\tilde{f}^* + ju\tilde{p}^* + jv\tilde{q}^* = 0, \\ (u^2+v^2)\tilde{f} - ju\tilde{p} - jv\tilde{q} = 0. \end{cases}$$

- Adding the above 2 equations together, then substracting the second one from the first one, this results in:

$$\begin{cases} (u^2+v^2)(\tilde{f}+\tilde{f}^*) + ju(\tilde{p}^*-\tilde{p}) + jv(\tilde{q}^*-\tilde{q}) = 0, \\ (u^2+v^2)(\tilde{f}-\tilde{f}^*) + ju(\tilde{p}^*+\tilde{p}) + jv(\tilde{q}^*+\tilde{q}) = 0. \end{cases}$$

Global methods

Fourier transform

- Solving the previous equations except for $(u, v) \neq (0, 0)$ ([Frankot and Chellappa, 1988]):

Frankot Chellappa relation

$$\tilde{f}(u, v) = \frac{-ju\tilde{p}^* - jv\tilde{q}^*}{u^2 + v^2}$$

Global methods

Fourier transform

- Solving the previous equations except for $(u, v) \neq (0, 0)$ ([Frankot and Chellappa, 1988]):

Frankot Chellappa relation

$$\tilde{f}(u, v) = \frac{-ju\tilde{p}^{*} - jv\tilde{q}^{*}}{u^2 + v^2}$$

- What about the mean values of the gradients: $\tilde{p}(0, 0) = \bar{p}$ and $\tilde{q}(0, 0) = \bar{q}$?
- reconstruction of surfaces with a null mean slant

Global methods

Fourier transform

$$\begin{cases} p(x,y) = p_0(x,y) + \bar{p} \\ q(x,y) = q_0(x,y) + \bar{q} \end{cases}$$

- Integration process is linear:

$f(x,y) = f_0(x,y) + g(x,y)$ where $g(x,y) = x\bar{p} + y\bar{q}$

Global methods

Fourier transform

$$\begin{cases} p(x,y) = p_0(x,y) + \bar{p} \\ q(x,y) = q_0(x,y) + \bar{q} \end{cases}$$

- Integration process is linear:

$f(x,y) = f_0(x,y) + g(x,y)$ where $g(x,y) = x\bar{p} + y\bar{q}$

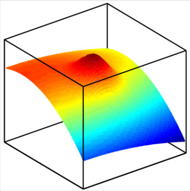

f

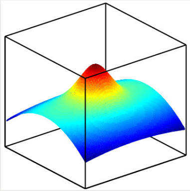

f_0

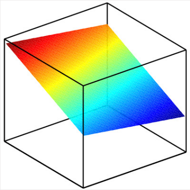

g

Comparisons

- Method

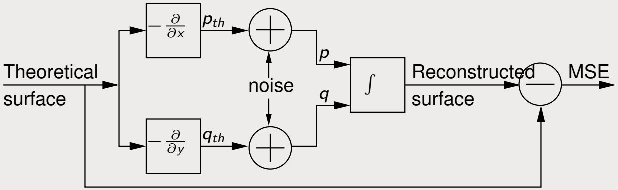

- Surfaces

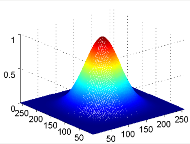

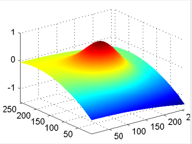

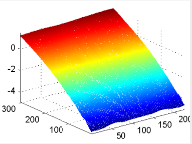

Comparisons

	kpix/s	Surf1	Surf2	Surf3
Coleman-Jain	410	0.1402	0.1016	0.0886
Rodehorst	82.1	0.0494	0.0535	0.1145
Gauss-Seidel 8N	0.1	0.0188		
SOR 8V	8.3	0.0162		
Frankot-Chellappa	145	0.0219	0.0193	0.0287
Karaçali-Snyder	20.8	0.0737	0.0909	0.1250

Further method to be investigated

More general approach of Height from Gradients

- Shape from [Polarization, Shading, Texture], Deflectometry require reconstructing a surface from an estimated gradient field

Further method to be investigated

More general approach of Height from Gradients

- Shape from [Polarization, Shading, Texture], Deflectometry require reconstructing a surface from an estimated gradient field

- Gradient processing [Agrawal and Raskar, 2007]

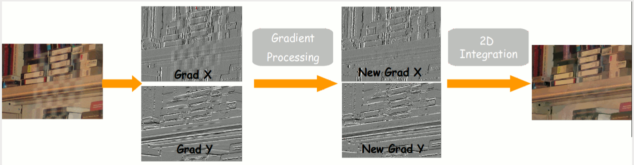

  - HDR compression, local illumination change, shadow removal, etc.

Further method to be investigated

More general approach of Height from Gradients

- Shape from [Polarization, Shading, Texture], Deflectometry require reconstructing a surface from an estimated gradient field
- Gradient processing [Agrawal and Raskar, 2007]

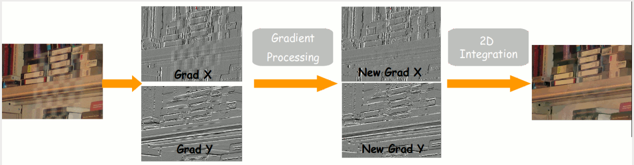

  - HDR compression, local illumination change, shadow removal, etc.

- The main problem remains: the gradients are generally non-integrable

Further method to be investigated

- Least squares formulation:

$$J(z) = \int\int \left((z_x - p)^2 + (z_y - q)^2 \right) dxdy$$

Further method to be investigated

- Least squares formulation:

$$J(z) = \int\int \left((z_x - p)^2 + (z_y - q)^2 \right) dxdy$$

- Extremum points are given by the Euler-Lagrange equation:

$$\frac{\partial J}{\partial z} - \frac{d}{dx}\frac{\partial J}{\partial z_x} - \frac{d}{dy}\frac{\partial J}{\partial z_y} = 0$$

Further method to be investigated

- Least squares formulation:

$$J(z) = \int \int \left((z_x - p)^2 + (z_y - q)^2 \right) dxdy$$

- Extremum points are given by the Euler-Lagrange equation:

$$\frac{\partial J}{\partial z} - \frac{d}{dx}\frac{\partial J}{\partial z_x} - \frac{d}{dy}\frac{\partial J}{\partial z_y} = 0$$

- Poisson equation is obtained by substituting J from (1) in (2):

$$0 - 2\frac{\partial}{\partial x}\left(z_x - p\right)) - 2\frac{\partial}{\partial y}\left(z_y - q\right) = 0$$

$$z_{xx} - p_x + z_{yy} - q_y = 0$$

$$\nabla^2 z = \mathrm{div}(p, q)$$

More general approach of Height from Gradients

- New functionnal J to minimize[Agrawal et al., 2009]:

$$J = \int\int E(z, p, q, z_x, z_y)dxdy$$

where E is a continuous differentiable function.

- By using Euler-Lagrange equations and considering the following form:

$$\begin{cases} \frac{\partial E}{\partial z_x} = f_1(z_x, z_y) - f_3(p, q) \\ \frac{\partial E}{\partial z_y} = f_2(z_x, z_y) - f_4(p, q) \end{cases}$$

where f_i are 4 different functions that should satisfy the integrability constraint $\frac{\partial^2 E}{\partial z_y \partial z_z} = \frac{\partial^2 E}{\partial z_z \partial z_y}$

More general approach of Height from Gradients

- New functionnal J to minimize[Agrawal et al., 2009]:

$$J = \int \int E(z, p, q, z_x, z_y) dxdy$$

where E is a continuous differentiable function.

- By using Euler-Lagrange equations and considering the following form:

$$\begin{cases} \frac{\partial E}{\partial z_x} = f_1(z_x, z_y) - f_3(p, q) \\ \frac{\partial E}{\partial z_y} = f_2(z_x, z_y) - f_4(p, q) \end{cases}$$

where f_i are 4 different functions that should satisfy the integrability constraint $\frac{\partial^2 E}{\partial z_y \partial z_z} = \frac{\partial^2 E}{\partial z_z \partial z_y}$

New formulation

$$\text{div}(f_1(z_x, z_y), f_2(z_x, z_y)) - \frac{\partial E}{\partial z} = \text{div}(f_3(p, q), f_4(p, q))$$

More general approach of Height from Gradients

- This generalized equation represent a continuum of solutions:
  - Poisson solver,
  - Frankot-Chelappa algorithm,
  - and more solutions

More general approach of Height from Gradients

- This generalized equation represent a continuum of solutions:
  - Poisson solver,
  - Frankot-Chelappa algorithm,
  - and more solutions

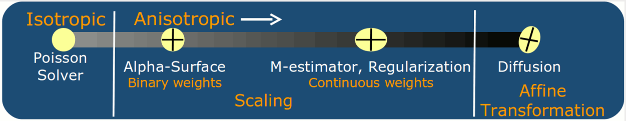

	$f_1(Z_x,Z_y)$	$f_2(Z_x,Z_y)$	$f_3(p,q)$	$f_4(p,q)$
Poisson solver	Z_x	Z_y	p	q
1.α-surface	$b_x Z_x$	$b_y Z_y$	$b_x p$	$b_y q$
2.M-estimators	$w_x Z_x$	$w_y Z_y$	$w_x p$	$w_y q$
3.Regularization	$w_x Z_x$	$w_y Z_y$	p	q
4.Diffusion	$d_{11} Z_x + d_{12} Z_y$	$d_{12} Z_x + d_{22} Z_y$	$d_{11} p + d_{12} q$	$d_{12} p + d_{22} q$

Outline

Experimental set-up

- Object to inspect:

- Experimental set-up:

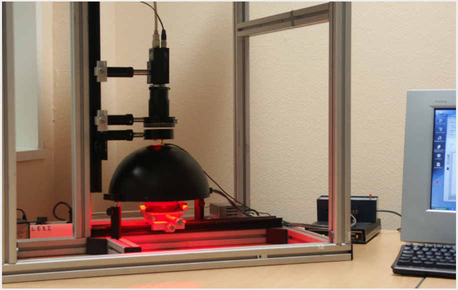

Software overview (LabVIEW)

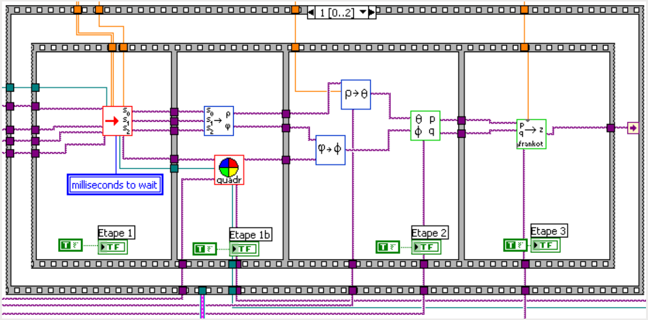

Software overview (LabVIEW)

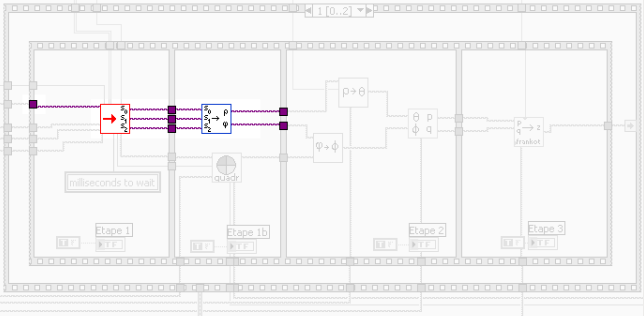

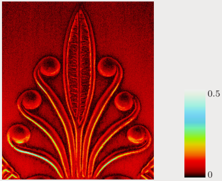

ρ

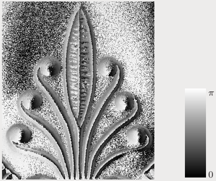

φ

- Time:
- 3.6s

Software overview (LabVIEW)

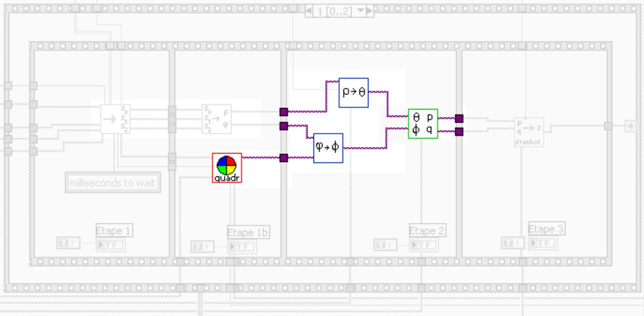

p

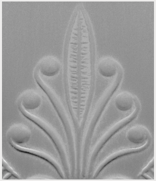

q

- Time:
- 3.6s
- 2.4s + 0.5s

Software overview (LabVIEW)

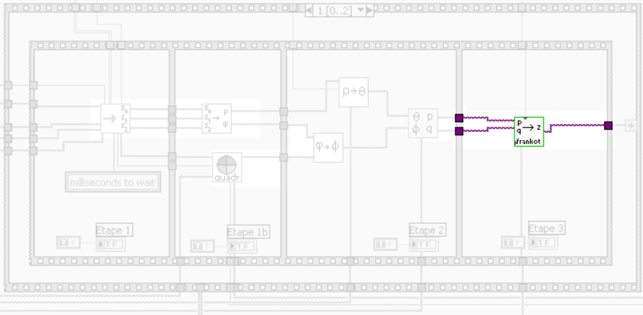

z

- Time:
- 3.6s
- 2.4s + 0.5s
- 1.2s

Software overview (LabVIEW)

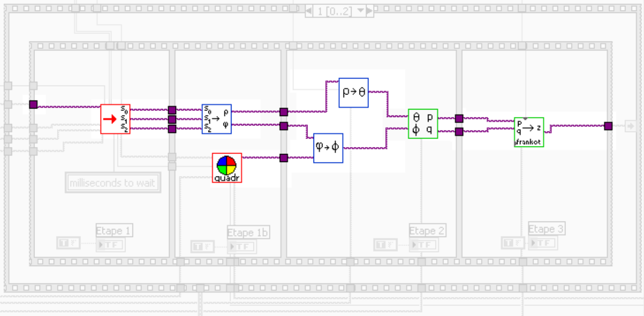

z

- Time:
- 3.6s
- 2.4s + 0.5s
- 1.2s

$\Rightarrow$ 7.7s

Calibration step

Constraint

The relationship between the degree of polarization ρ and the angle θ depends on the refractive index of the object.

- refractive index known
- calibration step

Calibration step

Constraint

The relationship between the degree of polarization ρ and the angle θ depends on the refractive index of the object.

- refractive index known
- calibration step

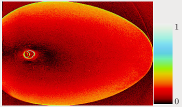

degree of polarization ρ

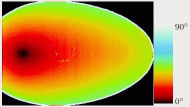

zenith angle θ

Calibration step

Constraint

The relationship between the degree of polarization ρ and the angle θ depends on the refractive index of the object.

- refractive index known
- calibration step

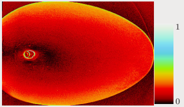

degree of polarization ρ

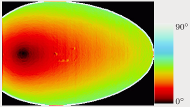

zenith angle θ

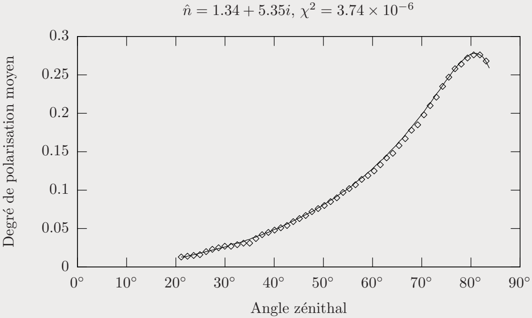

Quantitative evaluation of the method

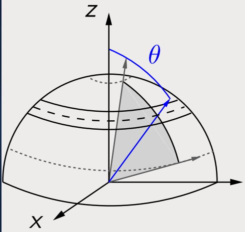

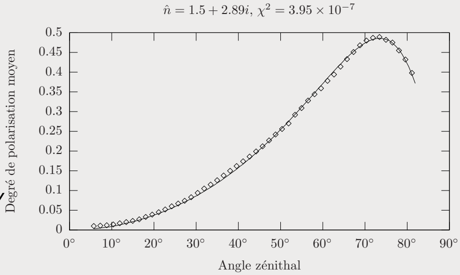

Quantitative evaluation of the method

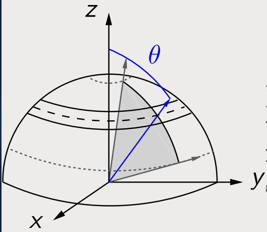

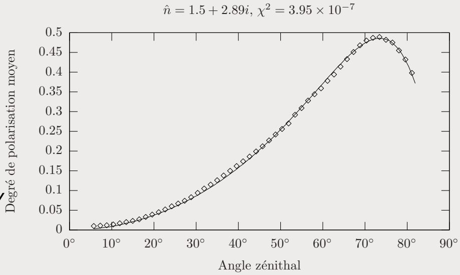

- Computed error: $\|\vec{e}\| = \|\vec{n}_{th} - \vec{n}_m\|$

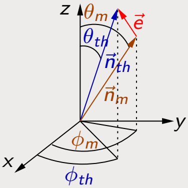

Quantitative comparisons

- Comparisons with the Replica and the Minolta scanners:

Quantitative comparisons

- Comparisons with the Replica and the Minolta scanners:



	Prototype	Replica	Minolta
$\|\|\vec{e}\|\|$	0.0572	0.0620	0.0765
θ	0.0239	0.0401	0.0455
ϕ	0.2359	0.1388	0.2554

Inspection

- Reference object:

- Object to inspect:

Inspection

- Reference object:

- Object to inspect:

- Map deviation:

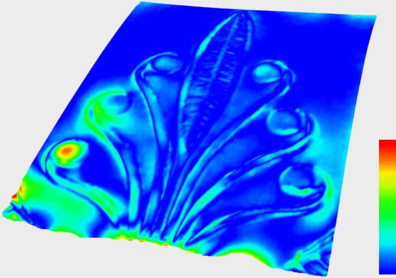

Brief conclusion

Pros

- 3D reconstruction of highly reflective surfaces
- Easy to implement (if the optical device is available)
- Sensitive to the surface gradients

Cons

- Refractive index is required or must be estimated
- Smooth surface (because of the integration process)
- The resolution cannot be estimated

Introduction

This work was initiated by the Ca.Vi.A.R. (Catadioptric VIsion for Aerial Robots) project: 2006-2009.

Catadioptric

- dioptric: science of refracting elements (lenses)
- catoptric: science of reflecting surfaces (mirrors)

- Evaluation of the panoramic vision contribution for aerial robots:

- Image processing applied to catadioptric image formation
- Calibration of catadioptric sensors
- 3D reconstruction, SLAM (Simultaneous Localization And Mapping)

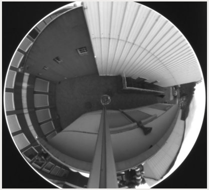

Main idea

PhD thesis

- Shape from Polarization applied to specular metallic surfaces
  - Mirrors used in Catadioptric sensors are specular
    $\hookrightarrow$ Try to use polarization imaging to provide useful information for the calibration process

Main idea

PhD thesis

- Shape from Polarization applied to specular metallic surfaces
    - Mirrors used in Catadioptric sensors are specular
      $\hookrightarrow$ Try to use polarization imaging to provide useful information for the calibration process

- Common calibration methods for omnidirectional catadioptric sensors assume that:
    1. mirror shape is perfectly known
    2. alignment of the sensor is perfect
    3. projection model can be easily parametrized

Main idea

PhD thesis

- Shape from Polarization applied to specular metallic surfaces
  - Mirrors used in Catadioptric sensors are specular
    $\hookrightarrow$ Try to use polarization imaging to provide useful information for the calibration process

- Common calibration methods for omnidirectional catadioptric sensors assume that:
  1. mirror shape is perfectly known
  2. alignment of the sensor is perfect
  3. projection model can be easily parametrized

- Relax these three constraints by using:
  - the generic concept developed by [Sturm, 2005]
  - polarization imaging

Polarization parameters of common mirrors

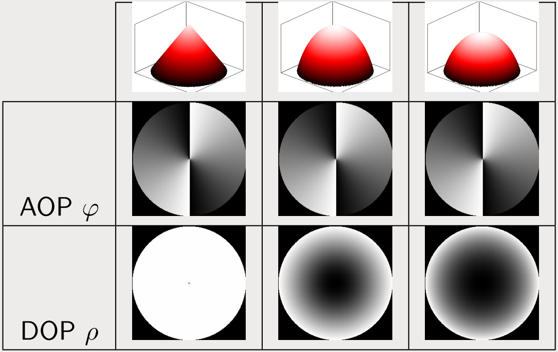

Recall of the relationship between the normals and the polarization parameters

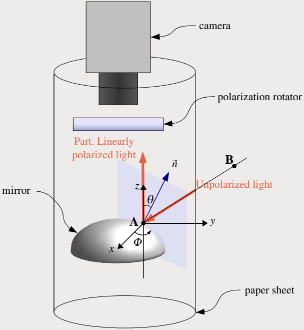

Required conditions

- Unpolarized lightning
- Highly reflective surface
- Telecentric lens

$$\vec{n} = \begin{pmatrix} p = \tan\theta\cos\phi \\ q = \tan\theta\sin\phi \\ 1 \end{pmatrix} \Rightarrow$$

(ϕ, θ) ?

Fresnel's coefficients

- Angle of polarization: $\varphi \Rightarrow \phi$
- Degree of polarization: $\rho \Rightarrow \theta$

Recall of the relationship between the normals and the polarization parameters

- From the degree of polarization ρ to the θ angle

$$\rho(\theta) = \frac{2n \tan\theta \sin\theta}{\tan^2\theta \sin^2\theta + |\hat{n}|^2}$$

- From the angle of polarization φ to the ϕ angle

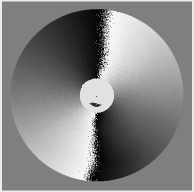

$$\phi = \varphi \pm \frac{\pi}{2}$$

$\Rightarrow$ambiguity in the determination of ϕ

How to solve the ambiguity ?

- computation of a segmented image I_{quad}:

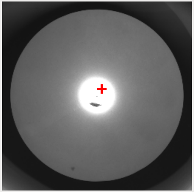

1. the center is approximately detected

How to solve the ambiguity ?

- computation of a segmented image I_{quad}:

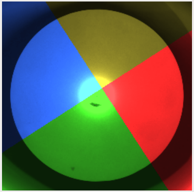

1. the center is approximately detected
2. the segmented image is created (orientation between 0 and $\pi/2$)

How to solve the ambiguity ?

- computation of a segmented image I_{quad}:

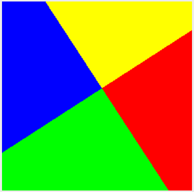

1. the center is approximately detected
2. the segmented image is created (orientation between 0 and $\pi/2$)
3. combination of the I_{quad} image and the φ image

- algorithm:

1. $\phi = \varphi - \pi/2$
2. $\phi = \phi + \pi$, if
   - $I_{quad} = 1$
   - $(I_{quad} = 3) \wedge (\phi \geq 0)$
   - $(I_{quad} = 0) \wedge (\phi \leq 0)$

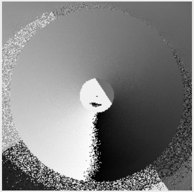

Non-parametric calibration

Generic concept

- [Sturm and Ramalingam, 2004]
- A camera is fully described by:
  - the coordinates of the rays (given in some local coordinate frame)
  - the mapping between rays and pixels (basically a simple indexing)

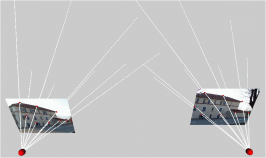

Sturm

Non-parametric calibration

Generic concept

- [Sturm and Ramalingam, 2004]
- A camera is fully described by:
  - the coordinates of the rays (given in some local coordinate frame)
  - the mapping between rays and pixels (basically a simple indexing)

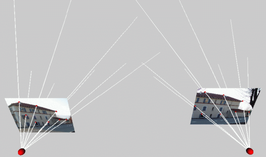

Sturm

- A light ray can be described by a pair of points:

$$\mathbf{A} = \begin{bmatrix} x_a & y_a & z_a \end{bmatrix}^T, \mathbf{B} = \begin{bmatrix} x_b & y_b & z_b \end{bmatrix}^T$$

Height computation

- Point **A** on the surface of the mirror:
  $\Rightarrow$ the 3D surface is computed by integrating the surface normals [Frankot and Chellappa, 1988] :

Frankot Chellappa

$$\tilde{f}(u,v) = \frac{-ju\tilde{p}^* - jv\tilde{q}^*}{u^2 + v^2}$$

Height computation

- Point **A** on the surface of the mirror:
  $\Rightarrow$ the 3D surface is computed by integrating the surface normals [Frankot and Chellappa, 1988] :

Frankot Chellappa

$$\tilde{f}(u, v) = \frac{-ju\tilde{p}^{*} - jv\tilde{q}^{*}}{u^2 + v^2}$$

- Example of reconstruction (hyperbolic mirror):

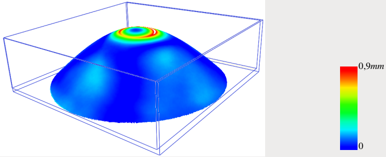

3D ray computation

- Point **B**:

$$\mathbf{B} = \mathbf{A} + k \begin{bmatrix} \tan 2\theta \cos\phi \\ \tan 2\theta \sin\phi \\ 1 \end{bmatrix}$$

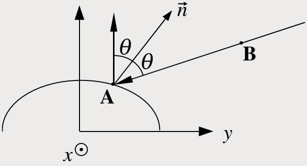

where k is a non-null constant

3D ray computation

- Point **B**:

$$\mathbf{B} = \mathbf{A} + k \begin{bmatrix} \tan 2\theta \cos\phi \\ \tan 2\theta \sin\phi \\ 1 \end{bmatrix}$$

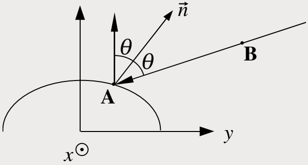

where k is a non-null constant

- Triangulation:

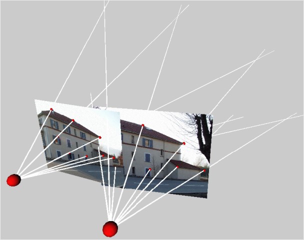

Simulation of the 3D reconstruction error

1. Give 3D points
2. Compute points reflected on the mirror
3. Simulate polarization calibration (noise added on the parameters)
4. Triangulate and compute the average error reconstruction
    - Linear Eigen method
    - Mid-Point method

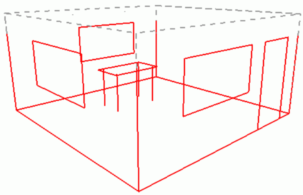

Simulation of the 3D reconstruction error

1. Give 3D points
2. Compute points reflected on the mirror
3. Simulate polarization calibration (noise added on the parameters)
4. Triangulate and compute the average error reconstruction
   - Linear Eigen method
   - Mid-Point method

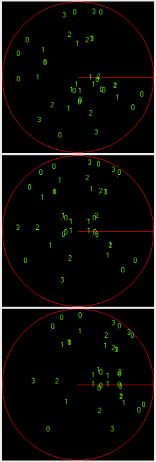

Simulation of the 3D reconstruction error

1. Give 3D points
2. Compute points reflected on the mirror
3. Simulate polarization calibration (noise added on the parameters)
4. Triangulate and compute the average error reconstruction
   - Linear Eigen method
   - Mid-Point method

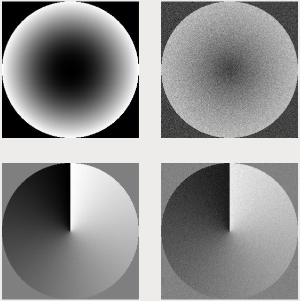

Simulation of the 3D reconstruction error

1. Give 3D points
2. Compute points reflected on the mirror
3. Simulate polarization calibration (noise added on the parameters)
4. Triangulate and compute the average error reconstruction
   - Linear Eigen method
   - Mid-Point method

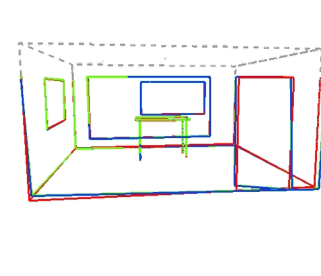

Influence of the polarization parameters measurement

- Calibration by polarization imaging
  - the two angles θ and ϕ are measured
  - the height z of the mirror is computed by integration
- Parameters used for the simulation
  - misalignment of 7 degrees
  - 100 reconstructions of the scene for each noise level
- Average error reconstruction of the scene
  - without the shape of the mirror (no integration process)
  - with the shape of the mirror (with integration process)

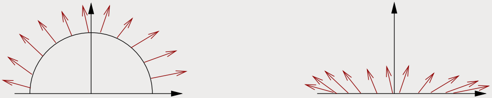

[Morel and Fofi, 2007]

Reconstruction error

induced by noisy measurement of the θ angle

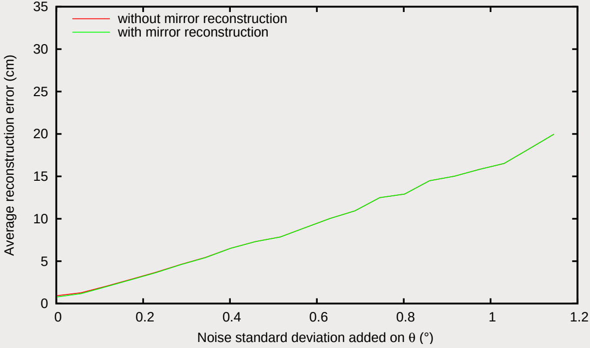

Reconstruction error

induced by noisy measurement of the ϕ angle

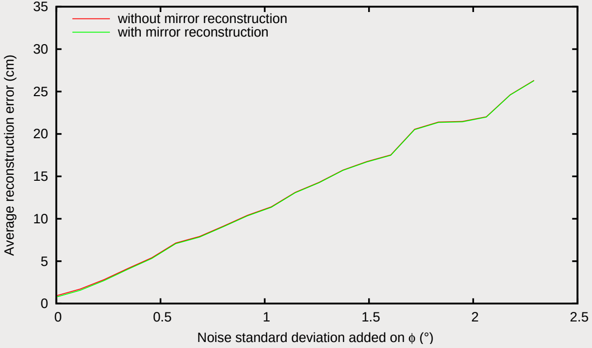

Reconstruction error

induced by noisy computation of the mirror height z

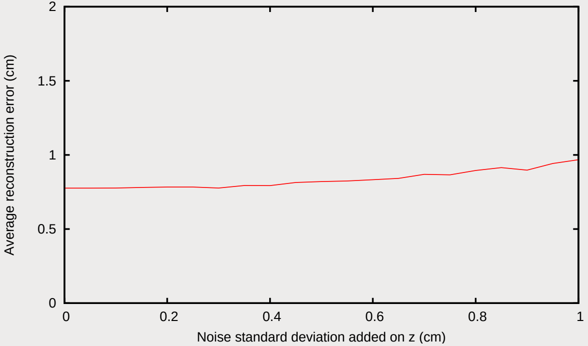

Indoor scene

- Catadioptric system on a 4 axis stage:

- x $[0, 1370mm]$
- y $[0, 990mm]$
- z $[0, 440mm]$
- θ $[-160, 160]$

3D reconstruction of some interest points

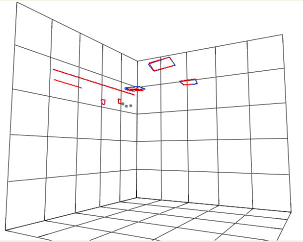

Hyperbolic mirror

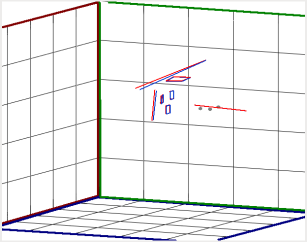

Spherical mirror

3D reconstruction of some interest points

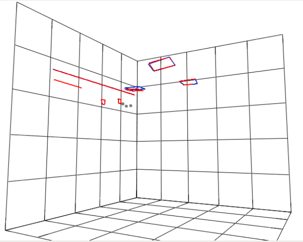

Hyperbolic mirror

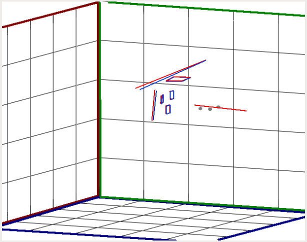

Spherical mirror

Reconstruction errors due to:

- small displacement of the sensor in the scene
- points are manually selected
- "direct" triangulation

Outdoor scene

Mensi© 3D scanner used to:

- locate the catadioptric sensor
- provide a ground truth map

Outdoor scene

Mensi© 3D scanner used to:

- locate the catadioptric sensor
- provide a ground truth map

Outdoor scene

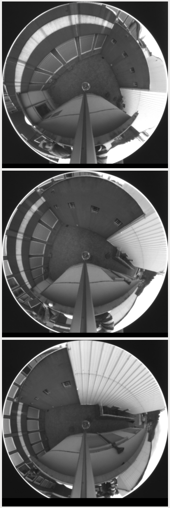

Conclusion

- Polarimetric cameras are increasing applications of polarization imaging
  - Robotics
  - Medical imaging

Conclusion

- Polarimetric cameras are increasing applications of polarization imaging
  - Robotics
  - Medical imaging
- Polacatadioptric sensor

Polarization by reflection

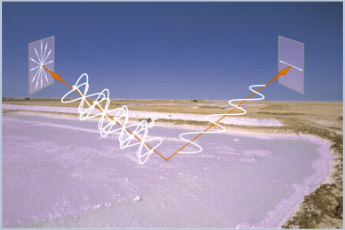

⇒ Outdoor water hazard detection

Polarization by scattering

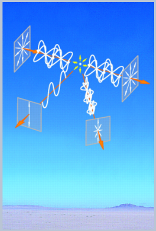

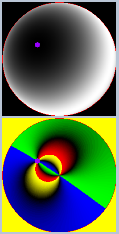

⇒attitude estimation (such as bees)

Conclusion

More applications in Robotics

- Polarization by reflection: road tracking

- Polarization by scattering: coarse depth estimation [Schechner et al., 2003]

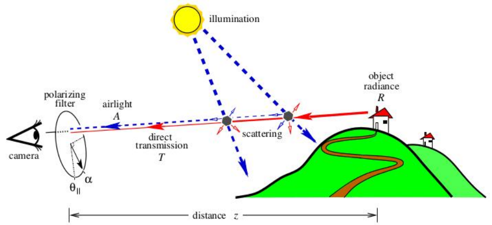

Bibliography I

Agrawal, A. and Raskar, R. (2007).
Gradient domain manipulation techniques in vision and graphics.
ICCV course.

Agrawal, A., Raskar, R., and Chellappa, R. (2009).
Surface reconstruction from gradient fields via gradient transformation.
International Journal of Computer Vision.

Alouini, M., Dolfi, D., Grisard, A., Lallier, E., Goudail, F., and Réfrégier, P. (2004).
Imagerie polarimétrique et multispectrale active : vers la détection et la reconnaissance d'objets de très faible contraste.
In *GDR Journées Imagerie Polarimétrique*.

Anastasiadou, M., Martino, A. D., Clement, D., Liège, F., Laude-Boulesteix, B., Quang, N., Dreyfuss, J., Huynh, B., Nazac, A., Schwartz, L., and Cohen, H. (2008).
Polarimetric imaging for the diagnosis of cervical cancer.
physica status solidi (c), 5(5):1423–1426.

Bibliography II

Atkinson, G. and Hancock, E. R. (2006).
Recovery of surface orientation from diffuse polarization.
IEEE Trans. Image Processing, 15(6):1653–1664.

Bolle, R., Connell, J., Haas, N., Mohan, R., and Taubin, G. (1996).
Veggievision: A produce recognition system.
In *Workshop on Applications of Computer vision*, pages 244–251.

Born, M. and Wolf, E. (1999).
Principles Of Optics.
Cambridge, 7 edition.

Chen, H. and Wolff, L. (1998).
Polarization phase based method for material classification in computer vision.
International Journal of Computer Vision, 28(1):73–83.

Bibliography III

Clark, J., Trucco, E., and Wolff, L. (1997).
Using light polarization in laser-scanning.
Image and Vision Computing, 15(2):107–117.

De Martino, A. and Laude-Boulesteix, B. (2004).
Polarimètre de mueller, imageur à cristaux liquides.
In *GDR Journées Imagerie Polarimétrique*.

Frankot, R. and Chellappa, R. (1988).
A method for enforcing integrability in shape from shading algorithms.
IEEE Trans. Pattern Analysis and Machine Intelligence, 10(4):439–451.

Horn, B. and Brooks, M. (1986).
The variational approach to shape from shading.
Computer Vision Graphics and Image Processing, 33(2):174–208.

Bibliography IV

Ikeuchi, K. (1983).
Constructing a depth map from images.
In *MIT AI Memo*.

Jacques, S. L., Ramella-Roman, J. C., and Lee, K. (2002).
Imaging skin pathology with polarized light.
Journal of Biomedical Optics, 7(3):329–340.

Kalayjian, Z., Andreou, A.G.and Wolff, L., and Sheppard, N. (1996).
A polarization contrast retina that uses patterned iodine-doped pva film.
In *European Solid-State Circuits Conference*, pages 308–311, Neuchatel, Switzerland.

Kalayjian, Z., Andreou, A.G.and Wolff, L., and Sheppard, N. (1997).
1d polarization retina.
Electronic Letters, 33(1):38–40.

Bibliography V

Karaçali, B. and Snyder, W. (2003).
Reconstructing discontinuous surfaces from a given gradient field using partial integrability.
Computer Vision and Image Understanding, 92(1):78–111.

Koshikawa, K. (1979).
A polarimetric approach to shape understanding.
In *International Joint Conference on Artificial Intelligent*, pages 493–495, Tokyo, Japan.

Kovesi, P. (2003).
Shapelets correlated with surface normals produce surfaces.
Technical report, School of Computer Science & Software Engineering.

Miyazaki, D., Kagesawa, M., and Ikeuchi, K. (2004).
Transparent surface modeling from a pair of polarization images.
IEEE Trans. Pattern Analysis and Machine Intelligence, 26(1):73–82.

Bibliography VI

Miyazaki, D., Saito, M., Sato, Y., and Ikeuchi, K. (2002).
Determining surface orientations of transparent objects based on polarization degrees in visible and infrared wavelengths.
Journal of the Optical Society of America A, 19(4):687–694.

Morel, O. and Fofi, D. (2007).
Calibration of catadioptric sensors by polarization imaging.
In *IEEE International Conference on Robotics and Automation*, Roma, Italy.
ACTi C 07- 37.

Morel, O., Stolz, C., Meriaudeau, F., and Gorria, P. (2006).
Active lighting applied to 3d reconstruction of specular metallic surfaces by polarization imaging.
Applied Optics, 45(17):4062–4068.
ACL C 06- 6.

Bibliography VII

Nayar, S. K. (1997).
Catadioptric omnidirectional camera.
In *CVPR '97: Proceedings of the 1997 Conference on Computer Vision and Pattern Recognition (CVPR '97)*, page 482, Washington, DC, USA. IEEE Computer Society.

Rahmann, S. (2003).
Reconstruction of quadrics from two polarization views.
In *Iberian Conference on Pattern Recognition and Image Analysis (IbPRIA03), Springer, LNCS 2652, Mallorca, Spain*, pages 810–820.

Ropars, G., Gorre, G., Floch, A. L., Enoch, J., and Lakshminarayanan, V. (2011).
A depolarizer as a possible precise sunstone for viking navigation by polarized skylight.
Proceedings of The Royal Society.

Bibliography VIII

Saito, M., Sato, Y., Ikeuchi, K., and Kashiwagi, H. (1999).
Measurement of surface orientations of transparent objects using polarization in highlight.
Journal of the Optical Society of America, 16(9):2286–2293.

Schechner, Y., Kiryati, N., and Basri, R. (2000).
Separation of transparent layers using focus.
International Journal of Computer Vision, 39(1):25–39.

Schechner, Y. Y., Narasimhan, S. G., and Nayar, S. K. (2003).
Polarization-based vision through haze.
Applied O, 42(3):511–525.

Sturm, P. (2005).
Multi-view geometry for general camera models.
In *IEEE Computer Vision and Pattern Recognition*, volume 1, pages 206–212, Washington, DC, USA. IEEE Computer Society.

Bibliography IX

Sturm, P. and Ramalingam, S. (2004).
A generic concept for camera calibration.
In *European Conference on Computer Vision*, volume 2, pages 1–13, Prague, Czech Republic. Springer.

Terrier, P. and Devlaminck, V. (2001).
A self calibrated image acquisition system for polarization estimation.
In *International Conference on Physics in Signal and Image Processing*, Marseille, France.

Tyo, J. (1998).
Optimum linear combination strategy for an n-channel polarization-sensitive imaging or vision system.
Journal of the Optical Society of America A, 15(2):359–366.

Bibliography X

Tyo, J. (2000).
Noise equalization in stokes parameter images obtained by use of variable-retardance polarimeters.
Optics Letters, 25:16.

Tyo, J., E.N. Pugh, J., and Engheta, N. (1998).
Colorimetric representation for use with polarization-difference imaging of objects in scattering media.
Journal of the Optical Society of America A, 15(2):367–374.

Vedel, M., Breugnota, S., and N., L. (2011).
Full stokes polarization camera.
In *SPIE Optical Engineering and Applications*, volume 8160.

Wallace, A., Liang, B., Trucco, E., and Clark, J. (1999).
Improving depth image acquisition using polarized light.
International Journal of Computer Vision, 32(2):87–109.

Bibliography XI

Wolff, L. B. and Andreou, A. (1995).
Polarization camera sensors.
Image and Vision Computing, 13(6):497–510.

Wolff, L. B. and Boult, T. E. (1991).
Constraining object features using a polarization reflectance model.
IEEE Trans. Pattern Analysis and Machine Intelligence, 13(7):635–657.

Wolff, L. B., Mancini, T. A., Pouliquen, P., and Andreou, A. G. (1997).
Liquid crystal polarization camera.
IEEE Trans. Robotics and Automation, 13(12):195–203.